

# NAVAL POSTGRADUATE SCHOOL

## Monterey, California



### THESIS

#### PSYCHOPHYSICAL COMPARISONS IN IMAGE COMPRESSION ALGORITHMS

by

Christopher J. Bodine

March 1999

Thesis Advisors:  
Second Reader:

William K. Krebs  
Lyn R. Whitaker

Approved for public release; distribution is unlimited.

19990512 026

# REPORT DOCUMENTATION PAGE

Form Approved  
OMB No. 0704-0188

Public reporting burden for this collection of information is estimated to average 1 hour per response, including the time for reviewing instruction, searching existing data sources, gathering and maintaining the data needed, and completing and reviewing the collection of information. Send comments regarding this burden estimate or any other aspect of this collection of information, including suggestions for reducing this burden, to Washington headquarters Services, Directorate for Information Operations and Reports, 1215 Jefferson Davis Highway, Suite 1204, Arlington, VA 22202-4302, and to the Office of Management and Budget, Paperwork Reduction Project (0704-0188) Washington DC 20503.

<b>1. AGENCY USE ONLY (Leave blank)</b>		<b>2. REPORT DATE</b> March 1999	<b>3. REPORT TYPE AND DATES COVERED</b> Master's Thesis
<b>4. TITLE AND SUBTITLE</b> PSYCHOPHYSICAL COMPARISONS IN IMAGE COMPRESSION ALGORITHMS			<b>5. FUNDING NUMBERS</b>
<b>6. AUTHOR(S)</b> Bodine, Christopher J.			
<b>7. PERFORMING ORGANIZATION NAME(S) AND ADDRESS(ES)</b> Naval Postgraduate School Monterey, CA 93943-5000			<b>8. PERFORMING ORGANIZATION REPORT NUMBER</b>
<b>9. SPONSORING / MONITORING AGENCY NAME(S) AND ADDRESS(ES)</b>			<b>10. SPONSORING / MONITORING AGENCY REPORT NUMBER</b>
<b>11. SUPPLEMENTARY NOTES</b> The views expressed in this thesis are those of the author and do not reflect the official policy or position of the Department of Defense or the U.S. Government.			
<b>12a. DISTRIBUTION / AVAILABILITY STATEMENT</b> Approved for public release; distribution is unlimited.			<b>12b. DISTRIBUTION CODE</b>
<b>13. ABSTRACT (maximum 200 words)</b> <p>Battlefield commanders are now requesting real-time visual battlefield information. These requests place an enormous strain on current transmission resources due to the file size of the images. As more and more visual information is sent, the ability to compress images efficiently becomes a significant issue. This thesis investigates whether any of the new image compression algorithms (Radiant TIN, Titan ICE, or Low Bit Rate) achieve higher compression ratios than the National Imagery Transmission Format Standard currently used by the Department of Defense. Titan ICE was found to perform better than Radiant TIN; however, the difference is not statistically significant. The Navy already has the proprietary rights to Radiant TIN. Therefore, in the absence of statistical significance, Radiant TIN is the recommended image compression algorithm for future use by the Department of Defense.</p>			
<b>14. SUBJECT TERMS</b> Human Systems Interface; Command, Control and Communications; Computing and Software			<b>15. NUMBER OF PAGES</b> 127
			<b>16. PRICE CODE</b>
<b>17. SECURITY CLASSIFICATION OF REPORT</b> Unclassified	<b>18. SECURITY CLASSIFICATION OF THIS PAGE</b> Unclassified	<b>19. SECURITY CLASSIFICATION OF ABSTRACT</b> Unclassified	<b>20. LIMITATION OF ABSTRACT</b> UL

NSN 7540-01-280-5500

Standard Form 298 (Rev. 2-89)  
Prescribed by ANSI Std. Z39-18



Approved for public release; distribution is unlimited

**PSYCHOPHYSICAL COMPARISONS IN IMAGE COMPRESSION  
ALGORITHMS**

Christopher J. Bodine  
Lieutenant, United States Navy  
B.S., Oregon State University, 1991  
B.A., Oregon State University, 1991

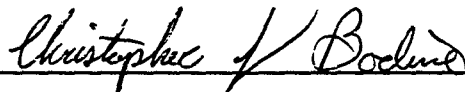
Submitted in partial fulfillment of the  
requirements for the degree of

**MASTER OF SCIENCE IN OPERATIONS RESEARCH**

from the


**NAVAL POSTGRADUATE SCHOOL  
March 1999**

Author:

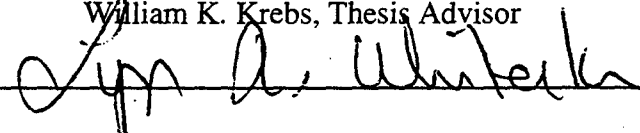


Christopher J. Bodine

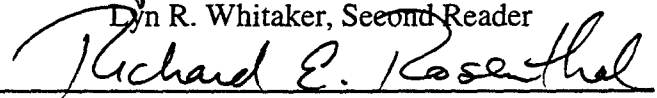
Approved by:



William K. Krebs, Thesis Advisor



Lyn R. Whitaker, Second Reader



Richard E. Rosenthal, Chairman  
Department of Operations Research



## **ABSTRACT**

Battlefield commanders are now requesting real-time visual battlefield information. These requests place an enormous strain on current transmission resources due to the file size of the images. As more and more visual information is sent, the ability to compress images efficiently becomes a significant issue. This thesis investigates whether any of the new image compression algorithms (Radiant TIN, Titan ICE, or Low Bit Rate) achieve higher compression ratios than the National Imagery Transmission Format Standard currently used by the Department of Defense. Titan ICE was found to perform better than Radiant TIN; however, the difference is not statistically significant. The Navy already has the proprietary rights to Radiant TIN. Therefore, in the absence of statistical significance, Radiant TIN is the recommended image compression algorithm for future use by the Department of Defense.



## **DISCLAIMER**

The reader is cautioned that the computer programs developed in this research may not have been applied to all cases of interest. While every effort has been made, within the time available, to ensure that the programs are free of computational and logical errors, they cannot be considered validated. Any application of these programs without additional verification is the risk of the user.





# TABLE OF CONTENTS

<b>I.</b>	<b>INTRODUCTION.....</b>	<b>1</b>
<b>II.</b>	<b>BACKGROUND.....</b>	<b>7</b>
	A. COLLECTION.....	7
	B. COMPRESSION BACKGROUND.....	11
	C. CATEGORIES OF COMPRESSION.....	14
	D. CURRENT STANDARD .....	17
<b>III.</b>	<b>LOSSLESS SCHEMES .....</b>	<b>19</b>
	A. HUFFMAN .....	19
	B. RUNLENGTH .....	20
	C. DIFFERENTIAL PULSE CODE MODULATION .....	20
<b>IV.</b>	<b>LOSSY SCHEMES .....</b>	<b>23</b>
	A. TRANSFORM CODING.....	23
	1. Coordinate Axes Rotations .....	23
	2. Basis Function Decompositions .....	24
	3. Discrete Cosine Transform.....	24
	4. Walsh-Hadamard Transform.....	26
	5. Symbolic.....	27
	6. Subband.....	27
	B. QUANTIZATION.....	28
	1. Lloyd-Max.....	28
	2. Vector Quantization .....	30
	3. Adaptive .....	31
<b>V.</b>	<b>ALGORITHMS TESTED.....</b>	<b>33</b>
	A. RADIANT TIN .....	33
	B. INTERIM LOW BIT RATE .....	36
	C. TITAN ICE .....	37
	D. PURPOSE AND RATIONALE.....	39
<b>VI.</b>	<b>METHODS .....</b>	<b>41</b>
	A. GENERAL METHODS.....	41
	B. DETECTION .....	41
	1. Participants .....	41
	2. Apparatus .....	41
	3. Stimuli .....	42
	4. Procedure.....	43
	C. ACCURACY IN IDENTIFICATION TEST.....	44
	1. Subjects .....	44

2.	Apparatus .....	44
3.	Stimuli .....	45
4.	Procedure .....	47
D.	REACTION TIME IN IDENTIFICATION TEST .....	47
1.	Subjects .....	47
2.	Apparatus .....	47
3.	Stimuli .....	48
4.	Procedure .....	48
E.	PAIRED COMPARISON .....	48
1.	Subjects .....	48
2.	Apparatus .....	49
3.	Stimuli .....	49
4.	Procedure .....	49
<b>VII.</b>	<b>DATA ANALYSIS .....</b>	<b>51</b>
A.	DETECTION .....	51
1.	Accuracy .....	51
2.	Reaction Time .....	56
B.	ACCURACY IN IDENTIFICATION TEST .....	60
3.	Simple Images .....	60
1.	Complex Images .....	65
C.	REACTION TIME IN IDENTIFICATION TEST .....	70
1.	Simple Images .....	70
2.	Complex Images .....	73
D.	PAIRED COMPARISON .....	76
1.	Simple Images .....	78
2.	Complex Images .....	79
<b>VIII.</b>	<b>CONCLUSION .....</b>	<b>81</b>
<b>APPENDIX A.</b>	<b>TEST IMAGES .....</b>	<b>83</b>
A.	SIMPLE IMAGES .....	83
B.	COMPLEX IMAGES .....	87
<b>APPENDIX B.</b>	<b>BRADLEY-TERRY MODEL .....</b>	<b>93</b>
<b>REFERENCES .....</b>		<b>95</b>
<b>BIBLIOGRAPHY .....</b>		<b>97</b>
<b>INITIAL DISTRIBUTION LIST .....</b>		<b>101</b>

## LIST OF FIGURES

Figure 1 LOS imagery transmission strategy .....	10
Figure 2 SATCOM imagery transmission strategy .....	11
Figure 3 Relationship between lossless and lossy compression .....	15
Figure 4 Generic Image compression System .....	15
Figure 5 Generic Image Lossy Algorithm .....	16
Figure 6 NITF File Format .....	17
Figure 7 Differential Image Plot .....	22
Figure 8 Rotation Transform .....	24
Figure 9 Typical Eight level Lloyd-Max Quantizer Distrubution .....	30
Figure 10 Typical APIC coder .....	31
Figure 11 Radiant-Tin Spatial Transformation Flow Diagram .....	34
Figure 12 Radiant TIN Compression Algorithm .....	35
Figure 13 LBR System .....	36
Figure 14 pSNR .....	39
Figure 15 Max error .....	39
Figure 16 Proportion Correct by Each Factor, Detection .....	53
Figure 17 Proportion Correct by Compression Level and Target, Detection .....	54
Figure 18 Proportion Correct by Compression Level and Algorithm, Detection .....	54
Figure 19 Proportion Correct by Target and Algorithm, Detection .....	55
Figure 20 Proportion Correct by Compression Level, Algorithm and Target, Detection .....	56
Figure 21 Mean Reaction Time by Each Factor, Detection .....	58
Figure 22 Mean Reaction Time by Compression Level and Target, Detection .....	59
Figure 23 Mean Reaction Time by Target and Algorithm, Detection .....	59
Figure 24 Proportion Correct by Factor, Simple Background .....	61
Figure 25 Proportion Correct by Algorithm and Image Quality Factors, Simple Background .....	62
Figure 26 Proportion Correct by Algorithm and Object, Simple Background .....	63
Figure 27 Proportion Correct by Image Quality and Object, Simple Background .....	64
Figure 28 Proportion Correct by Image Quality and Algorithm, Simple Background .....	65
Figure 29 Proportion Correct by Factor, Complex Background .....	67
Figure 30 Proportion Correct by Object and Algorithm, Complex Background .....	68
Figure 31 Proportion Correct by Image Quality and Object, Complex Background .....	68
Figure 32 Proportion Correct by Image Quality and Algorithm, Complex Background .....	69
Figure 33 Linear Regression of Compression Ratio on Accuracy, Complex Images .....	70
Figure 34 Mean Reaction Time by Factor, Simple Background .....	71
Figure 35 Reaction Time by Algorithm, Simple Images .....	73
Figure 36 Main effects on Time .....	75
Figure 37 Reaction Time by Algorithm, Complex Images .....	76
Figure 38 Pairwise Comparison Scoring of Simple Images .....	79
Figure 39 Pairwise Comparison Scoring of Complex Images .....	80



## LIST OF TABLES

Table 1 Coefficient Arrangement.....	21
Table 2 Original Pixel Values .....	21
Table 3 Predicted Values of Pixels .....	21
Table 4 Difference in Pixel Values .....	22
Table 5 Original 8 x 8 Image Block.....	25
Table 6 Transformed 8 x 8 Block.....	25
Table 7 Typical Eight-Level Lloyd-Max Quantizer Distrabution .....	29
Table 8 ANOVA of Accuracy of Detection.....	52
Table 9 ANOVA of Reaction Time of Detection .....	57
Table 10 ANOVA of Accuracy of Simple Images .....	60
Table 11 Test Statistics for Paired Test of Accuracy .....	65
Table 12 ANOVA of Accuracy of Complex Images .....	66
Table 13 ANOVA of Reaction Time of Simple Images .....	71
Table 14 Test Statistics for Paired Test of Reaction Time.....	72
Table 15 ANOVA of Reaction Time of Complex Images.....	74
Table 16 Raw Data Matrixes.....	77
Table 17 Input Matrixes .....	77
Table 18 Bradley-Terry Sample Results .....	78
Table 19 Bradley-Terry Simple Image Scores.....	78
Table 20 Bradley-Terry Complex Image Scores.....	80



## LIST ACRONYMS

ANOVA	Analysis of Variance
APIC	Adaptive Perpetual Image Coder
bpp	Bits per Pixel
C4	Command, Control, Communication, and Computers
D/C	Discrete-to-Continuous-Spatial
DCT	Discrete Cosine Transform
DoD	Department of Defense
DPCM	Differential Pulse Code Modulation
EJV2010	Concept for Future Joint Operations, Expanding Joint Vision 2010
ICE	Titian ICE
IS	Information Superiority
ISR	Intelligence, Surveillance, and Reconnaissance
JCS	Joint Chiefs of Staff
JND	Just Noticeable Difference
JPEG	Joint Photographic Experts Group
JV2010	Joint Vision 2010-A Vision for the Future
LBR	Interim Low Bit Rate
LOS	Line of Sight
LUT	Look-up Table
MCE	Mission Control Element
MSE	Mean Square Error
MXF	Message Transfer Facility
N6	Director of Space Information Warfare Command and Control
NAS	National Academy of Sciences
NASA	National Aeronautics and Space Administration
NIMA	National Imagery and Mapping Agency
NITF	National Imagery Transmission Format Standard
pSNR	Peak Signal to Noise Ratio
RTN	Radiant TIN
UAV	Unmanned Aerial Vehicles
VRG	Vision Research Graphics
VQ	Vector Quantization
WHT	Walsh-Hadamard Transform





## EXECUTIVE SUMMARY

Communications or lack of communications between battlefield commanders and their subordinates plays an essential role in determining the outcome of many battles throughout history. As technology advances, battlefield communication evolves, and the information that battlefield commanders require to make decisions increases.

The Chairman of the Joint Chief of Staff's issued two concept papers, *Joint Vision 2010 (JV2010) - A Vision for the Future* and *EJV2010, Concept for Future Joint Operations, Expanding Joint Vision 2010*. JV2010 looks at improvements in communications and how they can be incorporated into the military to improve its overall capabilities. JV2010 and EJV2010 emphasize the extreme importance of information and the ability to access that information on the battlefield in the future of war fighting.

The realization of JV2010 and EJV2010 requires that each military unit commander possess near real-time information on all activities within his region of responsibility. JV2010 combines the capabilities of "Intelligence, Surveillance, and Reconnaissance (ISR)" and "Command, Control, Communication, and Computers (C4)" to acquire and assimilate the information needed to neutralize adversarial forces and effectively employ friendly forces. The task of distributing data is complicated by numerous factors including, but not limited to, time, non-homogeneous equipment (ranging from mainframes to hand-held computers), hostile atmospheric conditions, and finite bandwidth capacity. (JCS, 1996)

JV2010 and EJV2010 lay the groundwork for the development of communication systems to improve the ability of commanders to make timely and informed decisions on

the battlefield. The foundation for these new forces is the ability to communicate quickly and efficiently to achieve information superiority. Information superiority is the ability to collect, process, and disseminate an uninterrupted flow of information while exploiting or denying an adversary's ability to do the same. (JCS, 1997) Failure to achieve Information Superiority (IS) puts both the goals of JV2010 and EJV2010, and the future of the Services at risk.

In order to achieve information superiority, the time required to transfer information to the battlefield must be minimized. The use of digital imagery increases transfer times and reduces the efficiency of communication systems. Image compression algorithms are required to reduce the storage size of digital images and reduce the time required to transmit these images. The three compression algorithms examined in this thesis are designed to improve the ability of today's communication systems to transfer large digital images.

Lossy compression algorithms significantly reduce the transmission times and storage space required for digital imagery. This reduction of image file size is necessary to meet increasing imagery requirements without upgrading current systems throughout the military. Additionally, the military does not have a standard format for tactical imagery. The standardization of the image format will allow for seamless transfers of imagery during joint operations. Currently, the Director of Space Information Warfare Command and Control is evaluating these three lossy algorithms: Titian ICE (ICE), Interim Low Bit Rate (LBR), and Radiant TIN (RTN), to replace the current algorithm being used by the Navy. All three of these new algorithms can achieve compression

ratios in excess of 60 times the maximum compression ratio of the algorithm currently used by the Navy. The Navy has proprietary rights to the code for RTN; therefore, selecting either ICE or LBR will require additional funding. This thesis will help N6 to determine if RTN should be selected as the Navy's new compression algorithm, or ultimately the DoD's.

Four experiments compare the performance of the three tested algorithms. Reaction time and accuracy data is collected for target detection and identification testing using simple and complex background images. Additionally, pairwise subjective comparisons of image quality are collected. The simple background images consist of U.S. Navy ships at sea. The complex background images are of automobiles parked in a wooded area. The automobiles are partially occluded by the foliage to reduce the amount of information about the automobile in the image.

The algorithm and compression ratio does not affect the identification of ships in a simple background. There are large individual differences in the respective subjects' abilities to identify the ships. In attempting to identify ships, an increase towards greater accuracy could be gained by increasing training of the subjects. The identification of cars in the complex background shows that ICE performs best followed by RTN then LBR. However, there is no statistical significant difference between ICE and RTN. RTN consistently performs better than LBR in target detection. It also performs better than LBR in the identification and subjective rankings of both the complex and simple images. There is no statistical significant difference in reaction times based on compression

algorithms. The only result consistent throughout the reaction time testing is that as the compression ratios increase the subjects' reaction times slowed.

The results of subjective rankings of image quality are consistent across both the simple and complex background test images. ICE is the algorithm subjectively preferred over either of the other algorithms at all compression ratios. RTN is consistently preferred over LBR with the exception of the lowest compression ratios. This effect is also observed in the accuracy testing. The difference is LBR's ability to compress images with less noticeable changes at the lowest compression ratios and thus does not invalidate the overall preference of RTN.

ICE's overall performance is better than RTN; however, the difference between the two algorithms is not statistically significant. Additionally, the ICE compression software is limited by its graphical user interface of compression ratios of 100 to 1; RTN does not have this limitation. Furthermore, the Navy already has the proprietary rights to RTN. RTN is the recommended compression algorithm. Any future testing should include the NITF 2.0 standard that was released at the completion of this study, and ICE should be reevaluated if the 100 to 1 software limitation is removed.

## ACKNOWLEDGMENTS

The author would like to thank Professor William 'Kip' Krebs and Professor Lyn Whitaker for their guidance and expertise in completing this thesis. Special thanks to Prof. Robert Read, who modified the Bradley-Terry model to account for bias, and supplied the S-plus code. Additionally the author wants to thank Professor Nicholas Beser, and Associate Professor William Walton of Johns Hopkins University Applied Physics Laboratory for providing image compression support.



## **DEDICATION**

This thesis is dedicated to my parents, Michael and Margaret Bodine, who thought I would never finish college after I enlisted in the Navy. A special thanks to my wife Heidi who's support and constant nagging kept me focused towards the completion of this thesis. I would also like to welcome Jonathan to our family, you have been a constant source of joy, even on the nights you refuse to sleep.





## I. INTRODUCTION

Communications or lack of communications between battlefield commanders and their subordinates have played an essential role in determining the outcome of many battles throughout history. As technology advances, battlefield communication evolves, and the information that battlefield commanders require to make decisions increases. Commanders are no longer content with a written synopsis of an area, but want to see near real-time imagery of the area. Due to the large amount of data required to encode an image and the limited speed at which data can be transferred with the current communication systems, image compression algorithms are required. This thesis is designed to help the Director of Space Information Warfare Command and Control (N6), compare three such image compression algorithms.

Early communications were limited to line of sight, using such methods as smoke signals, torches, flashing light, and semaphore flags (Holzman & Pehrson, 1995). In the 1790s, Napoleon used an optical telegraph, developed in 1793, to communicate with his commanders in the field. These optical telegraphs were stationed on hilltops throughout France and used articulated arms to encode messages and transmit them more than 5,000 kilometers. (National Academy of Sciences [NAS], 1997) The optical telegraph's limitation to line of sight was removed with the invention of the electric telegraph in 1844, which could transmit beyond visible distances (Bray, 1995).

Radio began to replace the electric telegraph when Guglielmo Marconi demonstrated in 1895 that radio can be detected over great distances (Masini, 1996). In

World War I, radio played an important role when both sides cut telegraphic cables to disrupt the flow of communications. Both the German and the British militaries used radios to communicate during World War I. In 1940 during World War II, the first hand-held radio was issued to the troops. This allowed mobile units to coordinate over large areas and revolutionized warfare. In 1957, the Soviet Union launched Sputnik, demonstrating the capability of space based communication systems. The first U.S. military satellite was launched in 1966 by the U.S. Air Force and was capable of both digital voice and data communications (NAS, 1997). The U.S. military continues to improve upon these original satellites and places new and more powerful satellites in orbit, improving communications on the battlefield.

In July of 1996, The Chairman of the Joint Chief of Staff's issued a concept paper, *Joint Vision 2010 (JV2010) - A Vision for the Future*. JV2010 looks at improvements in communications and how they can be incorporated into the military to improve its overall capabilities. In May of 1997, to further define the direction in which the armed forces should focus their developments and plans for the future, the Joint Chiefs issued EJV2010, *Concept for Future Joint Operations, Expanding Joint Vision 2010*. JV2010 and EJV2010 emphasize the extreme importance of information and the ability to access that information on the battlefield in the future of war fighting. The information by itself is insufficient; soldiers on the battlefield must have the ability to obtain the required information and have it when they need it. (Joint Chiefs of Staff [JCS], 1996) (JCS, 1997)

The Navy, along with the other services, is adjusting force structures toward a network centric battle force, reliant on the concept of having real-time battlefield and situational awareness through informational awareness. Wireless communication is the enabling technology allowing network-centric warfare to be achieved. According to Sun Tzu, if you know the enemy and know yourself, you need not fear the result of a hundred battles. If you know yourself but not the enemy, for every victory gained you will also suffer a defeat. (Handel, 1992)

The realization of JV2010 and EJ2010 requires that each military unit commander possess near real-time information on all activities within his region of responsibility. JV2010 combines the capabilities of "Intelligence, Surveillance, and Reconnaissance (ISR)" and "Command, Control, Communication, and Computers (C4)" to acquire and assimilate the information needed to neutralize adversarial forces and effectively employ friendly forces. The task of distributing data is complicated by numerous factors including, but not limited to, time, non-homogeneous equipment (ranging from mainframes to hand-held computers), hostile atmospheric conditions, and finite bandwidth capacity. (JCS, 1996)

Briggs and Goldberg (1995) demonstrate in their study the need for timely and accurate information. The study looks at military operations in the Persian Gulf during Desert Storm. Their findings show that 35 of 148, or 24%, of the U.S. casualties and 72 of 467, or 15%, of U.S. injuries resulted from misidentification "friendly fire." American forces destroyed 27 of 35, nearly 80%, of the U.S. M1 Abrams tanks and Bradley Fighting Vehicles. This is significant given that Iraqi canon fire could not penetrate

American tanks. The difficulty in identifying friendly forces is not new to the electronic battlefield, but the consequences are deadlier and faster. Clausewitz states that the difficulty of accurate recognition constitutes one of the most serious sources of friction in war (Handel, 1992).

As the battlefield becomes more complex, and decisions concerning deadly force are made at an ever-increasing rate, information about both one's own forces and the enemy's is needed to prevent "friendly fire." The speed at which the commander in the field receives the data can be the difference between destroying a "friendly tank" or being shot by the enemy while waiting for the information. The extreme cost of incorrectly identifying a target strongly influences the decision criteria of a commander on the battlefield. In a tactical situation, there is a strong bias to identify a vehicle as a foe, given any doubt. (Briggs & Goldberg, 1995)

JV2010 and EJV2010 lay the groundwork for the development of communication systems to improve the ability of commanders to make timely and informed decisions on the battlefield. The foundation for these new forces is the ability to communicate quickly and efficiently to achieve information superiority. Information superiority is the ability to collect, process, and disseminate an uninterrupted flow of information while exploiting or denying an adversary's ability to do the same. (JCS, 1997) Failure to achieve Information Superiority (IS) puts both the goals of JV2010 and EJV2010, and the future of the Services at risk.

In order to achieve information superiority, the time required to transfer information to the battlefield must be minimized. The use of digital imagery increases

transfer times and reduces the efficiency of communication systems. Image compression algorithms are required to reduce the storage size of digital images and reduce the time required to transmit these images. The three compression algorithms examined in this thesis are designed to improve the ability of today's communication systems to transfer large digital images.

Currently N6 is evaluating these three algorithms, Titan ICE (ICE), Low Bit Rate (LBR), and Radiant TIN (RTN), to replace the current algorithm being used by the Navy. All three of these new algorithms can achieve compression ratios in excess of 60 times the current maximum compression ratio of the algorithm used by the Navy. The Navy has proprietary rights to the code for RTN; therefore, selecting either ICE or LBR will require additional funding. This thesis will help N6 to determine if RTN should be selected as the Navy's new compression algorithm and ultimately the Department of Defense's (DoD).

The following chapters of this thesis are presented in the following order. Chapter II covers the driving forces behind the need for image compression algorithms. This chapter starts by presenting a few of the collection resources available in today's military followed by a brief history of the development of image compression algorithms. The two major categories of compression algorithms will be explained, concluding with the current DoD compression standard. Chapter III and Chapter IV describe the basic algorithms in each of the two major categories of compression algorithms. Chapter V describes the three algorithms tested in this thesis. The methods for testing these three algorithms are presented in Chapter VI, and the data analysis follows in Chapter VII.

The results of the data analysis and conclusions of this thesis are discussed in Chapter VIII.

## **II. BACKGROUND**

### **A. COLLECTION**

As technology and equipment continue to advance, digital information will be an integral part of operations in the battlefield. Although transmission equipment continues to improve and bandwidth capabilities are expected to be insignificant, these capabilities are also expected to fall short of transmission needs (González et al, 1994). There are several methods and devices capable of imaging the battlefield and transmitting the information to a collection agency. Each of these sources fills a very specific need in the information-gathering arena, though there are advantages and disadvantages to using each.

All the services are capable of collecting intelligence and imagery of one kind or another. The collection range of sophisticated imaging equipment is extensive, from equipment mounted on ships and land, to hand-held film and digital cameras. As computing power continues to increase, and the size of digital equipment continues to decrease, miniaturized, electronic-surveillance devices will increasingly be found on the battlefield.

With the invention of lighter-than-air vehicles and airplanes, information collection has moved to non-terrestrial sources. Today's reconnaissance aircraft have the ability to be tasked in real-time to meet current objectives of the operational commander. Additionally, these aircraft have higher resolution sensors, and are able to monitor at a region for extended periods of time. The disadvantage of aircraft is the risk to both man



and machine while flying over enemy-controlled areas. Aircraft are susceptible to being shot down or interdicted by the enemy during missions. Some of the aircraft currently in use are the U-2, the SR-71 Black Bird, the P-3 Orion, the TARPS equipped F-14 Tomcat, and Unmanned Aerial Vehicles (UAV).

With the launch of Intelsat-II (Early Bird) into a geosynchronous orbit in 1965, the United States entered into space-based communications. The DoD today has access to many space-based systems, both commercial and governmental. These sources include weather satellites, such as the Defense Meteorological Satellite Program, with the primary function of collecting weather data for operational forces. This satellite can provide real time tactical data, and circles the globe every 12 hours. Another is Landsat, a joint NASA/DoD platform capable of providing multi-spectral imagery. This system maps the surface of the earth, and spots man-made objects using both visible and infrared sensors. Finally, Lacrosse is a NASA system that uses Synthetic Aperture Radar orbiting in a low earth orbit.

These space-based collection systems were key in the planning and execution of the Gulf War. The satellites provided real-time weather information to aid the commanders in mission decision-making. The information from the satellites supported everything from the movement of individual aircraft to entire armored units, through the launch, en route, target, and recovery phases of their missions. (Muolo, 1993)

Some disadvantages of satellites include the problem of positioning the satellite above the intended target; whether or not the satellite can take pictures during daylight or nighttime; and how often the satellite is above the target. Additionally, the resolution of a

satellite image is usually not as defined as an image taken by an aircraft or a ground based sensor. Some advantages of satellites are that satellites are not vulnerable to being shot down by missiles; that satellites in geo-stationary orbits can stay above a target for an indefinite period of time; and that satellites provide images without placing pilots at risk.

The need for compression software, specifically image compression software for today's collection sources, is twofold. The first is the large number of bits required to represent an image digitally. The second is the reduced ability to receive large streams of data rapidly. Most collection sources have ground-based control units capable of receiving the vast quantities of information being transmitted. The re-transmitted imagery desired by the local commanders is limited by "bandwidth". The UAV for example has the capacity to transmit line of sight (LOS) to its Mission Control Element (MCE) at 137Mbits/sec. The commander on the ground can only receive between 1.5-10Mbits/sec (Figure 1), with most users limited to 1.5Mbits/sec. (Waller, 1996)

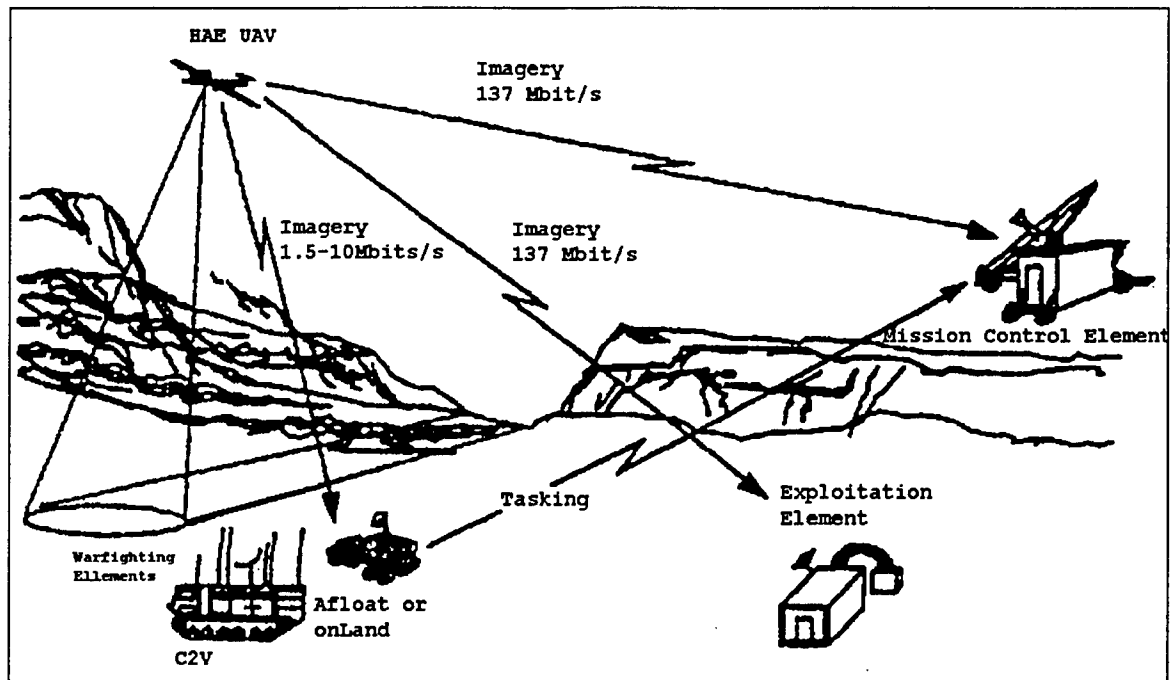


**Figure 1 LOS imagery transmission strategy**

When information has to be relayed via satellite, there is a reduction in the maximum capacity of data that can be transmitted to about 50Mbits/sec (Figure 2). A satellite relay is required any time the UAV is being operated beyond the LOS of the MCE. To overcome the limitations of bandwidth and reduce transmission time, it is mandatory to use methods to reduce the number of bits required to represent the required data in real time. (Waller, 1996)

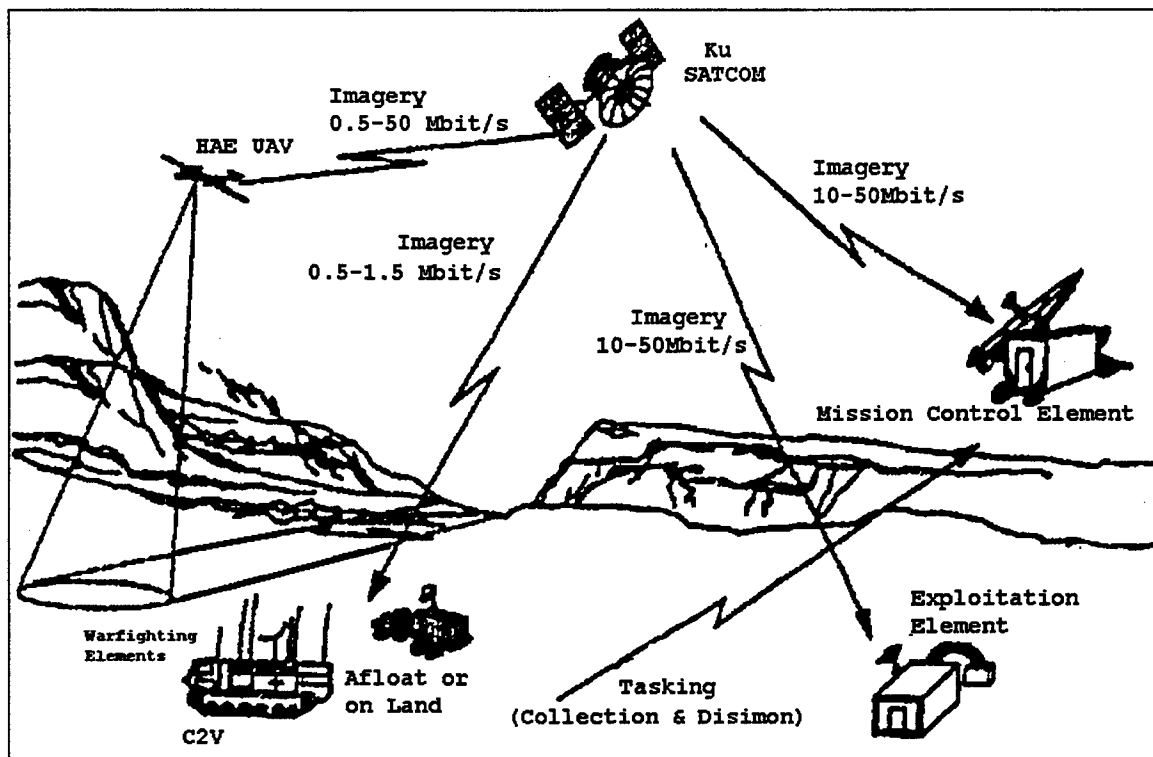


**Figure 2 SATCOM imagery transmission strategy**

The vast amount of digital data required to represent an image can best be demonstrated by transmitting a single image from LANDSAT. A single image comprised of approximately 6,000 X 6,000 pixels, each pixel composed of 8 bits, requires approximately  $2.9 \times 10^8$  bits of data (Rabbani & Jones, 1991), or approximately 280 Megabytes. The battlefield commanders would have to wait as long as 9 minutes for this single uncompressed image. The advantage of compression algorithms of 100 to 1 and above is that they can reduce the time required for the commanders to receive this LANDSAT information to less than six seconds.

## **B. COMPRESSION BACKGROUND**

Traditional compression schemes manipulate signal image pixel values based on mathematical formulas, without regard to the way the final reproduced signal is seen by a

human user. These mathematical functions are appropriate for some data, such as measurements or text, but it fails to take advantage of the characteristics of the human visual system. For example, if greater compression can be achieved, and the associated image quality loss is not perceivable to the human eye, then more of the data can be removed. Compression methods that take advantage of the nature of these phenomena are referred to collectively as "perceptual coding."

Perceptual coding can be accomplished through a variety of means. It usually involves using models of human perception, such as a human visual-system model. Computer vision models are becoming increasingly sophisticated in their attempt to emulate the human visual system. These new computational models are leading to models that are more accurate for Just Noticeable Difference (JND) and noise-masking. Hardware improvements have also increased to the point where practical digital signal processors can support perceptual coding. (Jayant, Johnston, & Safranek, 1993)

These models can be quite complex and their incorporation into compression algorithms is quite involved, requiring cooperation among psychologists, computer scientists, and engineers. The potential gains justify the development effort and have been estimated to yield 10-50% improvements in efficiency of compression, with no perceptual distortion. One approach is to transform the raw data, using a perceptual model, into features deemed important for perception. These features are then explicitly compressed and used to reconstruct the signal. Another approach is to incorporate perceptual knowledge into the computation of measurements of distortion and fidelity. These data are then used to produce computer code that will represent the image.

Regardless of the specific method, sensible incorporation of human perception is likely both to provide substantial improvements in compression performance, and to do so without significantly influencing tactical recognition.

Moeller and Hurlbert (1997) published a well-worded discussion of an important factor of target recognition. They discussed image segmentation as follows:

Recognizing and locating objects are fundamental tasks of the human visual system – but to determine ‘what’ is ‘where’, the visual system must first segment the image into regions likely to correspond to distinct objects. It is generally assumed that image segmentation, in which similar regions are grouped together and segregated from dissimilar regions, occurs at an early, preattentive level of visual processing (Moeller and Hurlbert, 1997, pp. 106).

This is an area where image coding can significantly influence recognition. At high levels of compression, most coding algorithms introduce distortion. This distortion appears in the form of blocked regions of reduced contrast and resolution. These regions may disrupt the preattentive level of visual processing and increase the probability of a false recognition or a miss.

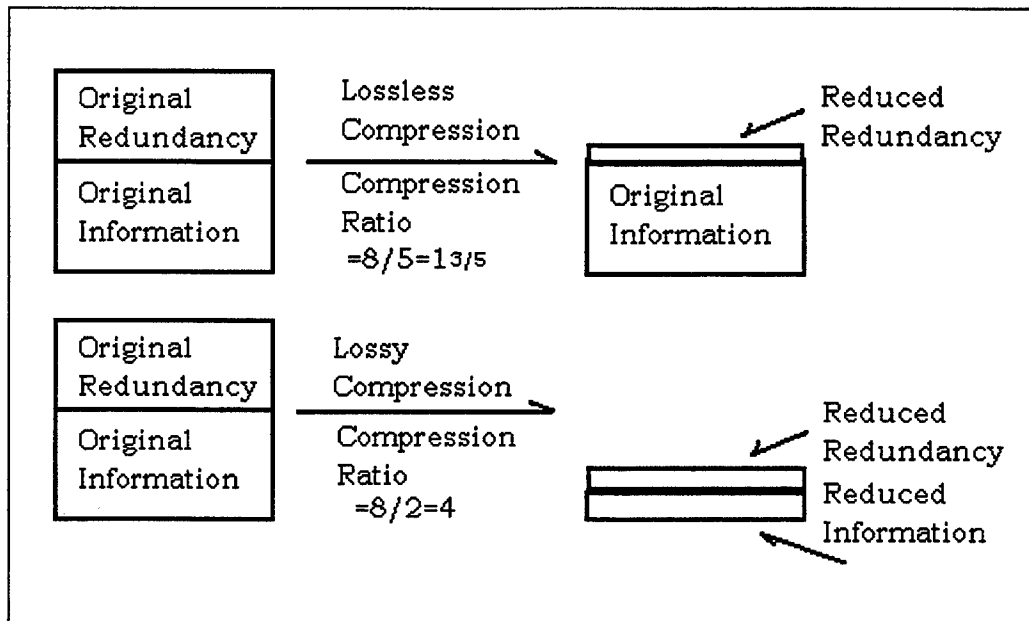
The study of “texture discrimination” is also closely related to image compression. Texture is the quality of a surface that gives the observer the feeling of a uniformly colored area caused by quasiperiodic repetitions of some patterns. (González et al, 1994) Texture-discrimination task performances depend on background noise. It is harder to find a texture with a noisy background than it is to find one without a noisy

background. Identical orientations of background noise and texture reduce performance. A simulation model for human texture-discrimination tasks shows that asymmetry, and the researchers concluded that the ability to differentiate texture from background increases with the variability in their orientation. (Caputo, 1996; Rubenstein & Sagi, 1990)

An image compression algorithm that does not consider the physiology of the visual system can mask targets. Masking occurs when distortion reaches levels that begin to blend foreground and background objects, thus decreasing texture variability.

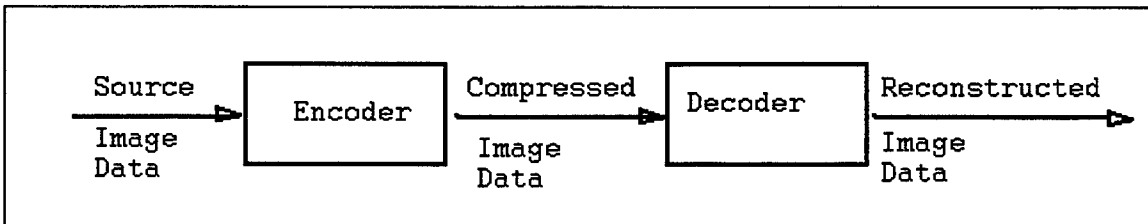
### **C. CATEGORIES OF COMPRESSION**

Image compression is divided into two major categories, “lossy” and “lossless”. A lossless compression algorithm is one that guarantees that its decompressed output is bit-for-bit identical to the original input. This is a much stronger claim than “visually indistinguishable from the original”. Lossy algorithms reduce the unnecessary redundancy the human eye is unable to perceive anyway. For most photo-like images, a large amount of data can be removed, while still maintaining most of the original visual features (Figure 3). (Beser, 1994)



**Figure 3 Relationship between lossless and lossy compression**

All image compression algorithms consist of two basic components, the encoder and the decoder (Figure 4). If the encoder retains all the information from the original image, the algorithm is lossless. Conversely, if it discards information to improve the compression ratio, it is a lossy algorithm.



**Figure 4 Generic Image compression System**

Lossy image compression techniques add an additional step when compressing an image. The additional step is quantization, where a reduced number of bits represents the transformed data (Figure 5). (Sanford, 1995)



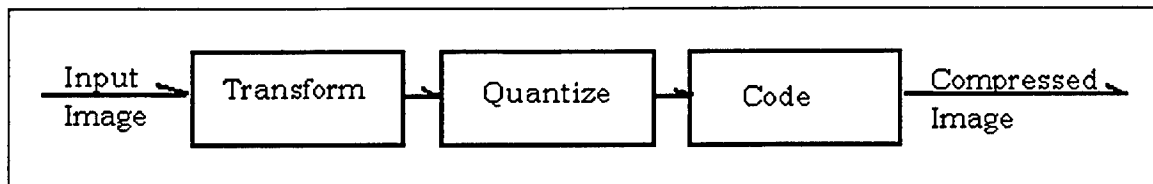


**Figure 5 Generic Image Lossy Algorithm**

Lossless algorithms are limited to a compression ratio bounded by the entropy of the image. This lower limit can be calculated from the number of bits that would be required to encode each pixel. The compression ratio can then be calculated by dividing the number of bits required to code all possible values of a pixel by the entropy of the image. For example, a gray scale image using eight bits to code each pixel (0 to 255) and an entropy of two bits per pixel, the maximum compression ratio attainable using a lossless compression algorithm, would be four to one. (Rabbani & Jones, 1991)

The evaluation of lossy compression algorithms has been done predominantly with mathematical tools. The most common calculation is to compute the mean square error (MSE) which is the average squared error between the original value of a pixel and the compressed value of that pixel. The peak signal-to-noise ratio (pSNR) and the maximum error between the uncompressed pixel value and the compressed value are also used. (Reiter, 1996) These numeric performance measures do not adequately describe image quality. An image that has good visual image qualities may have a high numerical error such as MSE. Algorithms that operate on spatial frequencies that are not sensitive to the human visual system may produce a large error while still being visually indistinguishable from the original. (Brower, 1994) With increased compression, a shift is required from traditional mathematical evaluation techniques to perceptual psychophysical performance measures.

#### D. CURRENT STANDARD

The current image compression algorithm in use by the United States Department of Defense is the National Imagery Transmission Format Standard (NITF), introduced in 1987. NITF is designed to work on low-cost workstations with limited power and storage space to send and receive data. The system design also accommodates for poor transmission lines that may include noise. (Brower, 1994) The Chairman of the Committee on Imagery Requirements and Exploitation directed the adoption of NITF by the Intelligence Community as the standard for image transfer in May 1989 (National Imagery and Mapping Agency [NIMA], 1999).

NITF is designed to transmit a file, composed of an image accompanied by sub-images, symbols, labels, text, and other information related to the image (NIMA, 1999). One main feature of NITF is that it allows for several items of each data type to be included in one file (Figure 6) (Paragon, 1999).

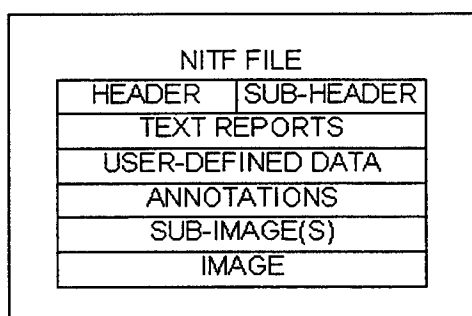


**Figure 6 NITF File Format**

The file is submitted to the Message Transfer Facility (MXF), which allows it to be transferred using any of the user-selectable protocols and media. The current image compression algorithm being used is a low-bit rate compression algorithm. The original standard is based on Joint Photographic Experts Group (JPEG) compression with pre-

and post-processing. The pre- and post-processing allow for compression ratios greater than 60, which is about the maximum achievable with standard JPEG. The “pre” and “post” are simple reduction routines, not part of a comprehensive compression algorithm. The inclusion of the added routines allows for the implementation of the system without developing a new standard.<sup>1</sup>

The following sections address different schemes for compressing images. The new algorithms being tested in this thesis are all derived from concepts and functions developed from these schemes. Lossless schemes will be discussed first, for they are implemented in the coding schemes of several of the lossy algorithms. The three algorithms being examined in this thesis are based on lossy schemes and will be discussed last. Any of the compression algorithms can be used by NITF due to the independence of NITF from the actual image format.

---

<sup>1</sup> The MXF functionality of the NITF software is not germane to this study and will not be addressed.

### **III. LOSSLESS SCHEMES**

All of the following lossless algorithms are based on variable-length code words. The use of variable-length code words allows for more efficient coding. The efficiency is gained by using the minimum number of bytes for each value being represented. These lossless schemes are used as part of the coding process for the lossy algorithms.

#### **A. HUFFMAN**

The Huffman encoding scheme is based on the probabilities of pixel value combinations appearing in the image. The probabilities for each combination of pixel values are calculated. The smallest code word is then assigned to the pixel-value combination that has the largest probability of appearing. The next smallest is then assigned the next most probable pixel value. This process is repeated until all possible pixel-value combinations are assigned a code word. The only rules for coding are first, no two characters will consist of identical codes, and second, each code will be constructed such that no additional indication is necessary to specify where a code begins and ends once the starting point is known (Huffman, 1952). This general process has been modified in two ways to increase the efficiency of the coding scheme.

The first modification is to reduce the code-word set by combining the least probable pixels into one code word. This is accomplished by using the code word for the combined pixel values followed by the value itself. If the probability of this combined code word is low, the overall savings to the complexity and storage requirements are decreased, without any significant decrease in the efficiency of the coding.

The second modification is to eliminate the need to make two passes of the image, one to calculate the probabilities of each pixel value, the next to code the values. Either calculating the probabilities from a small part of the image or using a standard probability table based on typical images can eliminate the second scan. (Rabbani & Jones, 1991) Images with a high correlation will have the greatest compression ratios.

## **B. RUNLENGTH**

The runlength coder is used to code the series of ones and zeros of a binary file. A symbol is used to indicate the start of a run followed by the number of instances. For example, if there are 92 consecutive occurrences of zero, the storage requirement is 184 bytes ( $92 \times 2 \text{ bytes/occurrences} = 184 \text{ bytes}$ ). By coding these zeros, the storage requirement is now 2 bytes for a compression ratio of 92 to 1. This runlength compression can then be coded using Huffman coding to increase the compression ratio by as much as three to one. (Reiter, 1996) The simplest implementation of this algorithm codes each individual line in the image with its own Huffman code. Higher order implementations take into account the previous lines in the image to develop the Huffman code table for those lines. These higher order implementations are more efficient, taking into account the vertical correlation of the image. (Rabbani & Jones, 1991)

## **C. DIFFERENTIAL PULSE CODE MODULATION**

The Differential Pulse Code Modulation (DPCM) is a predictive algorithm. There is a great degree of correlation between adjacent pixels in most images. Predictive algorithms use this tendency to estimate the value of the next pixel, then only encode the

difference in the predicted value and the actual value. This value is usually smaller than the original pixel value, thus reducing the number of bits required to store the information. The number of pixels used to estimate the next pixel is the order of the predictor. As the order increases, the accuracy of the estimate for the next pixel increases. There is a diminishing return on increasing the order of the predictor. For efficiency, most do not go past the third order. (Rabbani & Jones, 1991)

DPCM can be encoded either as a lossless or lossy algorithm. For this example, a third-order global predictor is used to predict pixel values in the image. The difference between the predicted value of the pixel and the actual value of the pixel is then stored. A simple polynomial can use the pixels to the left, upper left, and above to predict the next value. A, B, and C are arranged around x, the predicted value, Table 1.

B	C
A	x

**Table 1 Coefficient Arrangement**

With the polynomial  $0.75A - 0.5B + 0.75C$ , Table 2 can be converted into Table 3 with a difference Table 4. (Rabbani & Jones, 1991)

139	144	149	153
144	151	153	156
150	155	160	163
159	161	162	160

**Table 2 Original Pixel Values**

0	0	0	0
0	146.5	153	155
0	153.75	155.5	160.5
0	160.5	163.25	163.75

**Table 3 Predicted Values of Pixels**

139	144	149	153
144	4.5	0	1
150	1.25	4.5	2.5
159	.5	-1.25	-3.75

**Table 4 Difference in Pixel Values**

The distributions of coded values typically have a Laplacian Distribution with a mean of zero. The Laplacian Distribution of coded values also has a reduced variance increasing the ability to compress the image. (Figure 7) (Rabbani and Jones, 1991) If the images are to be coded as a lossy image, a quantizer is added to reduce the significance of each pixel value. By reducing the accuracy of the pixel values, a smaller range of numbers can be used to code these new values. With a smaller set of values, fewer bits can then be used to encode the remaining pixel values. This is the step where information about the image is lost. The coding of the prediction error rather than the data results in a higher quality reconstruction of the original image. (Venkataraman & Farrelle, 1994)

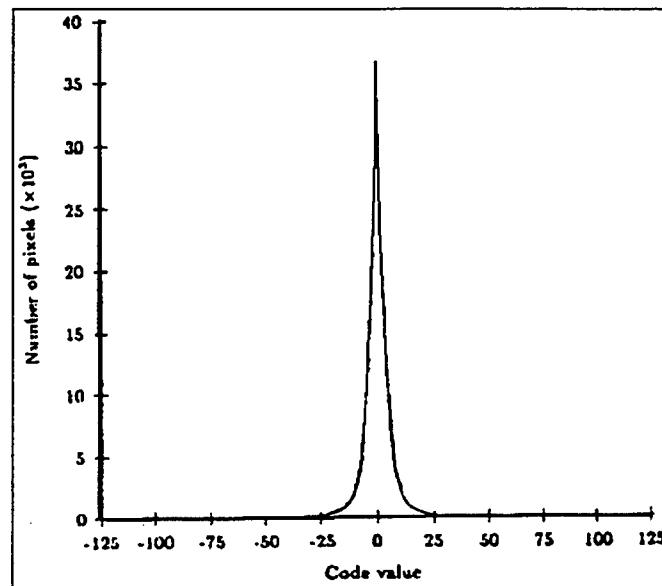


**Figure 7 Differential Image Plot**

## IV. LOSSY SCHEMES

The algorithms tested in this thesis, RTN, ICE, and LBR, are lossy algorithms. Lossy algorithms can achieve higher compression ratios by removing some of the information in the reconstructed images. The following lossy algorithms are the building blocks for the next generation of compression schemes.

### A. TRANSFORM CODING

Transform coding is applied to the images by first dividing the image into sub images or blocks. Each of these blocks then has the transform applied to it independent of all the other blocks. For example, the JPEG compression algorithm divides the image into 8X8 blocks. These 8X8 blocks are then transformed using a unitary transform. A unitary transform is a reversible linear transformation made of complete, orthonormal discrete-basis functions. (Rabbani & Jones, 1991) The unitary transform causes a reduction in the variance of the coefficient values. The remaining coefficients can then be coded in either a lossless or lossy algorithm.

#### 1. Coordinate Axes Rotations

Coordinate axes rotation takes advantage of the fact that there is high enough correlation between adjacent pixels to reduce the variance in the pixel intensity values. The majority of the correlations lie along a 45° diagonal (Figure 8). To reduce the MSE when coding the image, each sub-block of the image is rotated about the axes. Let  $\mathbf{X}=(x1,x2)$  and  $\mathbf{Y}=(y1,y2)$  represent the location of a pixel before and after the rotation respectively.

Then, 
$$\begin{bmatrix} y1 \\ y2 \end{bmatrix} = \frac{1}{\sqrt{2}} \begin{bmatrix} 1 & 1 \\ -1 & 1 \end{bmatrix} \begin{bmatrix} x1 \\ x2 \end{bmatrix}.$$
 To decode the image, the inverse



transform is applied to each of the previously transformed blocks:

$$\begin{bmatrix} x_1 \\ x_2 \end{bmatrix} = \frac{1}{\sqrt{2}} \begin{bmatrix} 1 & -1 \\ 1 & 1 \end{bmatrix} \begin{bmatrix} y_1 \\ y_2 \end{bmatrix}. \quad (\text{Rabbani \& Jones, 1991})$$

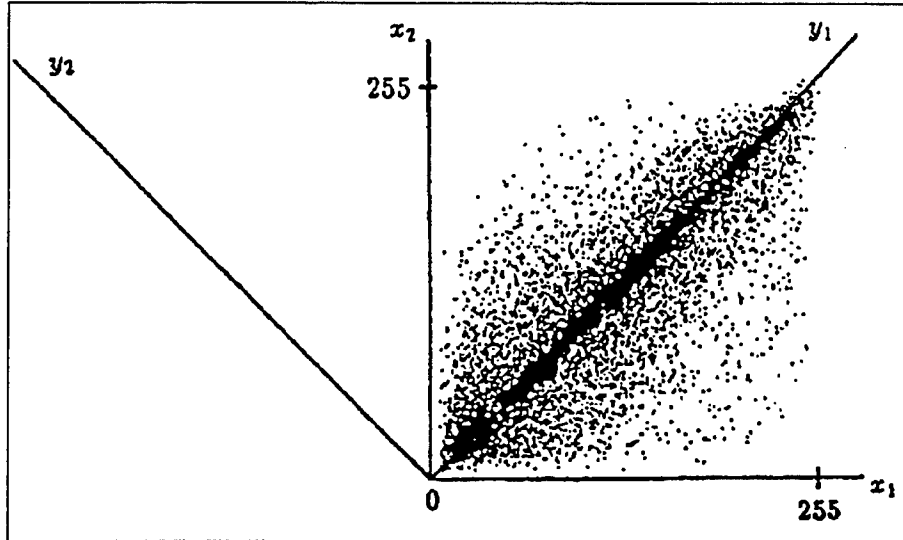


**Figure 8 Rotation Transform**

## **2. Basis Function Decompositions**

More generally, the above rotation is a transformation by a basis,  $\mathbf{Y}=\mathbf{AX}$  where  $\mathbf{A}$  is any basis. The decoder would then be  $\mathbf{X}=\mathbf{BY}$  where  $\mathbf{B}=\mathbf{A}^{-1}$ , and other basis can be used. These transformations are commonly used in discrete cosine transforms (discussed later), based on sines and cosines of different frequencies leading to spectral decomposition of the original image. (Rabbani & Jones, 1991)

## **3. Discrete Cosine Transform**

The most common frequency Transformation is the Discrete Cosine Transformation (DCT). Let the horizontal and vertical indices of the transformed block be  $u$  and  $v$ ; and the original horizontal and vertical indices of the block be  $j$  and  $k$ .  $F(u,v)$  is the pixel value at the position  $u, v$  in the transformed block and  $f(j,k)$  is the pixel value

at the position  $j,k$  in the original block.  $C(0) = \frac{1}{\sqrt{2}}$ , 1 otherwise. The DCT sub-divides the image into small, square blocks, and then uses the following transformation on each block:

$$F(u,v) = \frac{4C(u)C(v)}{n^2} \sum_{j=0}^{n-1} \sum_{k=0}^{n-1} f(j,k) \cos\left[\frac{(2j+1)u\pi}{2n}\right] \cos\left[\frac{(2k+1)v\pi}{2n}\right].$$

Table 5 is an example of an 8 x 8 block transformation using DCT, while Table 6 is the transformed block. The Inverse DCT is used to restore the original image and is defined as:

$$f(j,k) = C(u)C(v)F(u,v) \cos\left[\frac{(2j+1)u\pi}{2n}\right] \cos\left[\frac{(2k+1)v\pi}{2n}\right]. \text{ (Rabbani \& Jones, 1991)}$$

	J=0	J=1	J=2	J=3	J=4	J=5	J=6	J=7
K=0	139	144	149	153	155	155	155	155
K=1	144	151	153	156	159	156	156	156
K=2	150	155	160	163	158	156	156	156
K=3	159	161	162	160	160	159	159	159
K=4	159	160	161	162	162	155	155	155
K=5	161	161	161	161	160	157	157	157
K=6	162	162	161	163	162	157	157	157
K=7	162	162	161	161	163	158	158	158

**Table 5 Original 8 x 8 Image Block**

	U=0	U=1	U=2	U=3	U=4	U=5	U=6	U=7
V=0	315	0	-3	-1	1	-1	1	0
V=1	-6	-4	-2	-1	-1	0	0	0
V=2	-3	-2	-1	1	0	0	0	0
V=3	-2	-1	0	0	0	0	0	0
V=4	0	0	0	1	0	0	0	0
V=5	1	0	1	0	0	0	0	0
V=6	0	0	0	0	0	1	0	0
V=7	-1	1	1	-1	1	0	0	0

**Table 6 Transformed 8 x 8 Block**

JPEG image compression is an example of a DCT algorithm designed for compressing either full-color or gray-scale images of natural, real-world scenes. It works

well on photographs, naturalistic artwork, and similar material. It does not work as well on lettering, simple cartoons, or line drawings. JPEG is designed to exploit known limitations of the human eye, notably the fact that small color changes are perceived less accurately than small changes in brightness.

Typically, gray-scale images do not compress by large factors. Because the human eye is much more sensitive to brightness variations than to hue variations, JPEG can compress hue data more heavily than brightness (gray-scale) data. A gray-scale JPEG file is generally only about 10%-25% smaller than a full-color JPEG file of similar visual quality. However, the uncompressed gray-scale data is only 8 bits/pixel, or one-third the size of the color data; therefore, the calculated compression ratio is much lower. The threshold of visible loss is often around five to one compression for gray-scale images. The exact threshold at which errors become visible depends on the viewing conditions. The smaller an individual pixel, the harder it is to see an error; therefore errors are more visible on a computer screen (at 70 or so dots/inch) than on a high-quality color printout (300 or more dots/inch). Thus, a higher-resolution image can tolerate more compression. (JPEG Image compression FAQ, 1998)

#### **4. Walsh-Hadamard Transform**

The Walsh-Hadamard Transform (WHT) is not as efficient as the DCT algorithm but has the advantage of being simple to implement. All of the coefficients in the WHT basis are either +1 or -1. The basis can be recursively formed to generate any square matrix. (Rabbani & Jones, 1991)

## **5. Symbolic**

Symbolic Transformation is designed to code images with a man-made object in them. The image is transformed into a symbolic representation of the entire scene instead of pixels. Objects that are well defined by this algorithm are edges, arcs, and changes in texture. The background is coded separately from the objects coded by symbols. By coding the detail and texture separately, the algorithm benefits from both vector- and texture-coding strong points. Symbolic Transformation is designed to increase the detail of the reconstructed image to maintain more edge information and enhance the compressed image.

## **6. Subband**

These are frequency-sensitive compression algorithms. Each image is divided into separate images containing only specific frequency data. This division is accomplished with the use of high and low-band filters. The advantage to dividing the image into these separate subbands is that the different frequencies can be coded so that those that are most noticeable to the eye are not compressed as highly. Uniformly scaling the JND threshold controls the step sizes of the quantizer to control compression and/or perceptual quality. (González et al, 1994)

An example of a subband algorithm is a wavelet transformation. A wavelet transformation is a set of repeated one-dimensional high- and low-pass filters. The two equations that make up the filters are composed of a scaling function and a wavelet function. Wavelet compression can provide between 1.5 and 4 times better performance for a given image quality compared to JPEG. (Reiter, 1996)

One of the common outcomes of compression algorithms is a tiling or blocking effect in a compressed image. Many algorithms first divide the image into regions or blocks and then execute the compression routines on each block, causing the tiling effect.

An alternative method of compressing images at higher compression ratios is to use hierarchical coding, employing wavelet transformations. Typically, these reconstructed images, compressed using wavelets, do not exhibit the tile effect. In wavelet coders the image is usually recursively decomposed into several subbands which are then quantized. Optimal quantization for each of the subbands is not trivial in linear-phase wavelets since the subbands are not mutually orthogonal. (Venkataraman & Farrelle, 1994)

## **B. QUANTIZATION**

Quantization is the process of reducing the amount of data used to represent the image. Setting a threshold and removing all values that fail to meet the minimum required value is one method. An alternate method is to reduce the number of different values used in the data. By binning the data the number of unique pixel intensities is reduced.

### **1. Lloyd-Max**

Lloyd-Max Quantizer is a staircase function that first partitions input pixel values into  $N$  intervals with boundaries  $d_1, \dots, d_N$ . This quantizer then maps the original values into discrete values termed *reconstruction levels*  $r_1, \dots, r_N$ . The values are derived to minimize the expected square error  $D$  between the original pixel values and the transformed pixels:

$$D = \sum_{i=0}^{N-1} \int_{d_i}^{d_{i+1}} (e - r_i)^2 p_e(e) de, \quad (4.1)$$

where  $p_e(e)$  the distribution of the pixel values to be quantized. (Rabbani & Jones, 1991)

The solution to the equation (4.1) will yield decision levels “halfway between the neighboring reconstruction levels and reconstruction levels that lie at the center of the mass of the probability density enclosed by the two adjacent decision levels” (Rabbani and Jones, 1991, pp. 84), in particular

$$r_i = \frac{\int_{d_i}^{d_{i+1}} e p_e(e) de}{\int_{d_i}^{d_{i+1}} p_e(e) de}. \quad (4.2)$$

There is no closed form solution to equation 4.1. Numerical techniques must be used to estimate the solution. When the pixel data is successfully transformed, the transformed data now has a Laplacian density. A 3-bit quantizer can be used with the parameters listed in Table 7 and shown in Figure 9. (Rabbani & Jones, 1991)

i	$(d_i, d_{i+1}) \rightarrow r_i$	Probability
0	$(-255, -16) \rightarrow -20$	0.025
1	$(-16, -8) \rightarrow -11$	0.047
2	$(-8, -4) \rightarrow -6$	0.145
3	$(-4, 0) \rightarrow -2$	0.278
4	$(0, 4) \rightarrow 2$	0.283
5	$(4, 8) \rightarrow 6$	0.151
6	$(8, 16) \rightarrow 11$	0.049
7	$(16, 255) \rightarrow 20$	0.022

**Table 7 Typical Eight-Level Lloyd-Max Quantizer Distrabution**

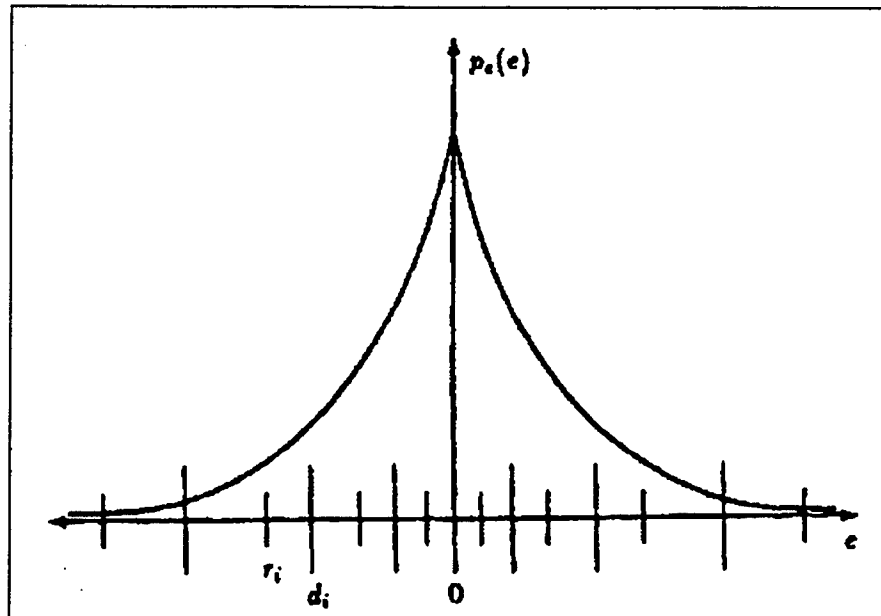


**Figure 9 Typical Eight level Lloyd-Max Quantizer Distribution**

## **2. Vector Quantization**

Vector Quantization (VQ) is a process for converting the image into vectors much like a symbolic algorithm. The symbols or vectors come from a 'codebook' of vectors, this codebook is generally developed by 'training.' Training of the codebook is accomplished by examining images similar to the images to be compressed. The more representative of the images the codebook is, the better the algorithm will perform. (Rabbani & Jones, 1991)

The image is divided into vectors, and then these vectors are coded from the codebook. A code and a location of the start of the vector in the original image now represent each vector in the original image. If the image does not use a predefined codebook, the codebook must be sent in addition to the compressed image. The VQ coders are theoretically optimal from the information point of view. However, as compression ratios are increased beyond one bit per pixel (bpp), the tile effect and

blocking artifacts are again observed in the reconstructed image. (Venkataraman & Farrelle, 1994) Vector quantization is the extreme case of symbolic transformation, but the textual information is not coded separately; it is all coded as edges. VQ is used for computer auto-identification. This algorithm is not used in any of the tested algorithms.

### 3. Adaptive

Most of the algorithms listed can be adaptive. The process of making them adaptive requires an additional pass through the image to optimize the coding of the coefficients. Adaptive algorithms attempt to eliminate the artifacts produced by most compression algorithms at high compression ratios. The most common artifact is tiling which is caused by the image being divided into blocks and then coded independently of the surrounding blocks. Adaptive DPCM reduces these effects by using the surrounding blocks as inputs for compressing each block. Frequency coding such as vector quantizations, also develops artifacts at high compression ratios, as previously stated.

An example of an adaptive subband coder is the Adaptive Perpetual Image Coder (APIC). With locally adaptive perpetual quantization it minimizes the perceptual distortion of the image. The quantization is based on an estimate of the amount of masking available for each subband coefficient. (Figure 10) (González et al, 1994)

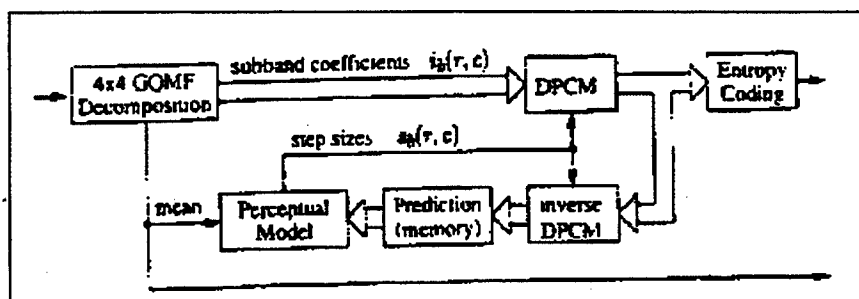


Figure 10 Typical APIC coder





## **V. ALGORITHMS TESTED**

### **A. RADIANT TIN**

RTN is a system of software tools designed to make imagery available at all levels of the military force-structure using low-bandwidth channels. The project's goals are to use existing hardware; provide high-ratio image compression with low file overhead; minimize or eliminate the need for added equipment; and to provide a simple, graphical user-interface. The RTN process uses a multi-step process to improve compression performance.

The first step in the compression process is to define the edges in the image. Each of the edges is coded into a vector consisting of a starting point and a path to the end of the edge. The second step is to compare the textures on either side of each of the edge vectors. The texture information allows for a texture gradient across each edge.

The information about the image is now coded using two different methods. The edge information is coded using a symbolic transform method. The remaining texture area is coded using a wavelet transform. The second method transforms spatial domain information using a residual error approach (Figure 11) (Beser, 1994). The Radiant TIN algorithm uses either symbolic decomposition or the frequency decomposition to achieve compression values more than 1 to 100 (Figure 12) (ISOA, 1995).

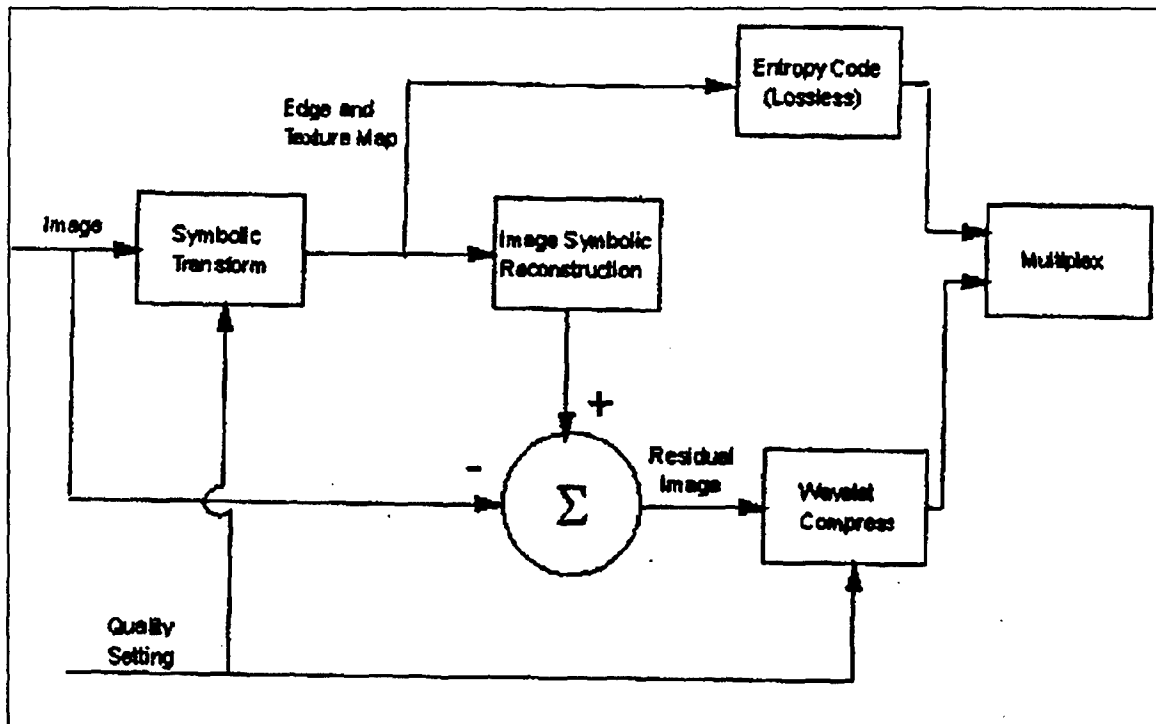


**Figure 11 Radiant-Tin Spatial Transformation Flow Diagram**

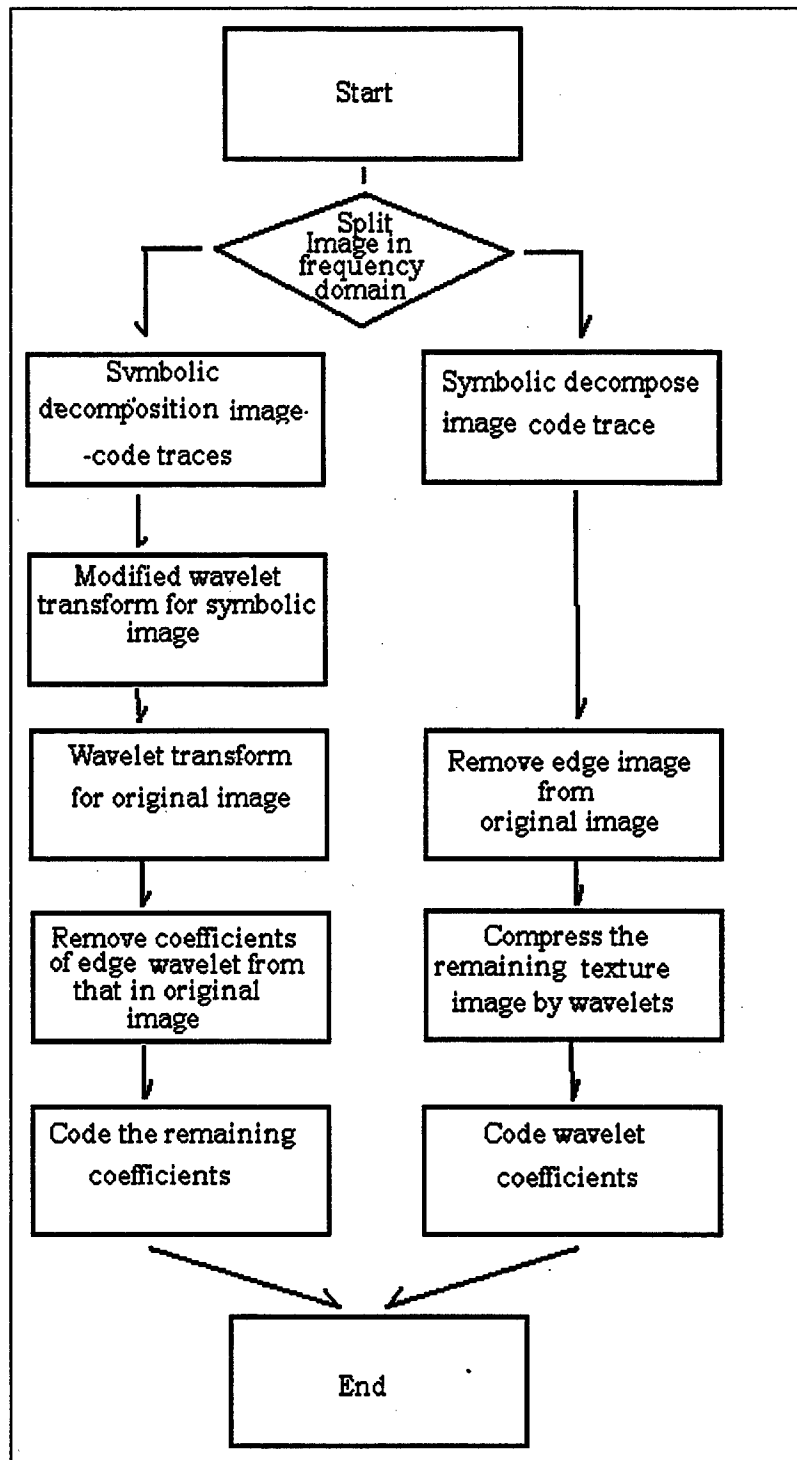


**Figure 12 Radiant TIN Compression Algorithm**

Sanford (1995) tests RTN against JPEG, Yuval Fisher's Fractal Compression Program, and Aware Corporation Wavelet compression algorithms. He concludes that JPEG does well at low compression ratios, while RTN does well at high compression ratios. Sanford's thesis employs both quantitative and qualitative testing for a difference in the algorithms. The qualitative evaluation consisted of a self-paced paired comparison test. The subjects' task was to choose the best image from the pair. Subjects rated the Wavelet image highest, followed by RTN.

## B. INTERIM LOW BIT RATE

LBR is a command-line compression algorithm based on the JPEG compression engine. LBR can increase the achievable compression ratios by downsampling the image before compressing it with a JPEG encoder. In the reconstruction phase, LBR upsamples the image after using the JPEG decoder (Figure 13). Downsampling the image causes the image to be blurred and introduces aliasing, while the JPEG encoder causes blocking at high compression ratios. LBR reduces these effects by adjusting the relative compression contributions from the two components. (Lan & Reitz, 1996)

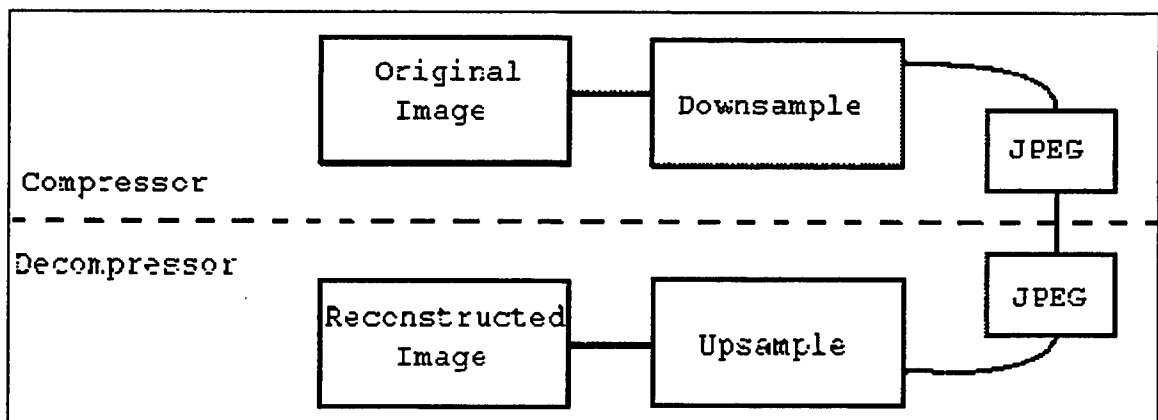


Figure 13 LBR System

The downsampling is based on the combination of a discrete-to-continuous-spatial (D/C) conversion and an anti-aliasing filter. These filters work as one filter by combining with each other through multiplication. The downsampling is performed on the rows of the image and then again on the columns of the image from the first downsampling. The upsampling is performed by first applying a D/C conversion to the compressed image and then resampling at a higher rate. This upsampling is performed in the reverse order of rows and columns as the downsampling is applied. The order of compressing the rows and columns may be reversed for software optimization. (Lan & Reitz, 1996)

### **C. TITAN ICE**

Titan ICE is based on a combination of wavelet and subband transformations. The algorithm is designed to compress radiological and other high-resolution digital imagery. These images are compressed to 30 to 1 while still maintaining sufficient quality to allow diagnostic readings (Reiter, 1996). The algorithm uses the JND threshold to adjust the compression equations to optimize the compression ratio at any compression quality. ICE uses the same algorithms for compression, but exceeds the JND threshold for lower quality levels in order to achieve the higher compression ratios. By coding each of the subbands independently with the wavelet transformation, ICE is able to reduce the perceptual errors introduced during coding.

ICE is a two-channel algorithm, which applies a low-pass filter of the rows of the image and then discards every other sample in the row. It then applies the high-pass filter on the rows of the image and discards every other sample. This process of filtering and

then downsampling is then applied to the columns of the image. The low-pass filter extracts the trends, whereas the high-pass filter extracts the detail. This is a single-level wavelet transform. This process may be repeated on any subband, but is usually done only on subbands that are formed from applying the filters and downsampling to both rows and columns. (Reiter, 1996)

Reiter using pSNR and Max error has done some comparative work between JPEG and Titan Ice. These results were also compared to those of qualitative measurements by human observers. Reiter acknowledges the need for perceptual measurements, but presented the mathematical results as a relative comparison. In the pSNR-to-compression graph (Figure 14), and the Max-error-to-compression-ratio graph (Figure 15), wavelet compression outperformed JPEG. In the perceptual testing subjects preferred the wavelet algorithm to JPEG even with identical pSNR. (Reiter, 1996)

Experiments using ICE and JPEG revealed that ICE has one half as many numeric errors as the JPEG compressed images. Additional experiments used the two algorithms to compress medical x-ray images for a subjective comparison. The compressed images were then examined by a radiologist who preferred ICE to JPEG. The medical image test concentrated on JND. (Reiter, 1996) The point at which each algorithm passes the JND threshold is a good indication of how each will perform at higher compression ratios.

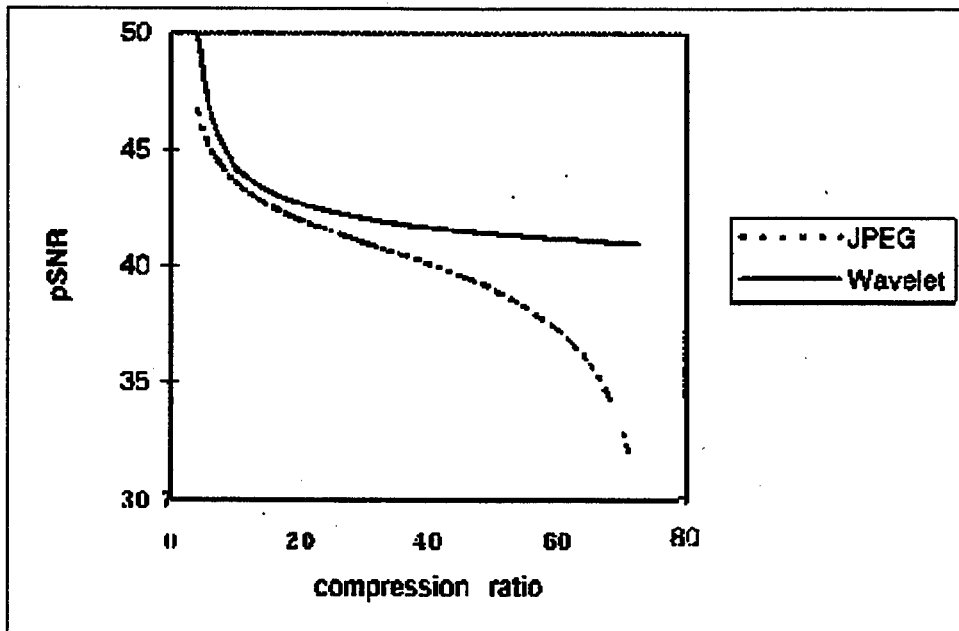


Figure 14 pSNR

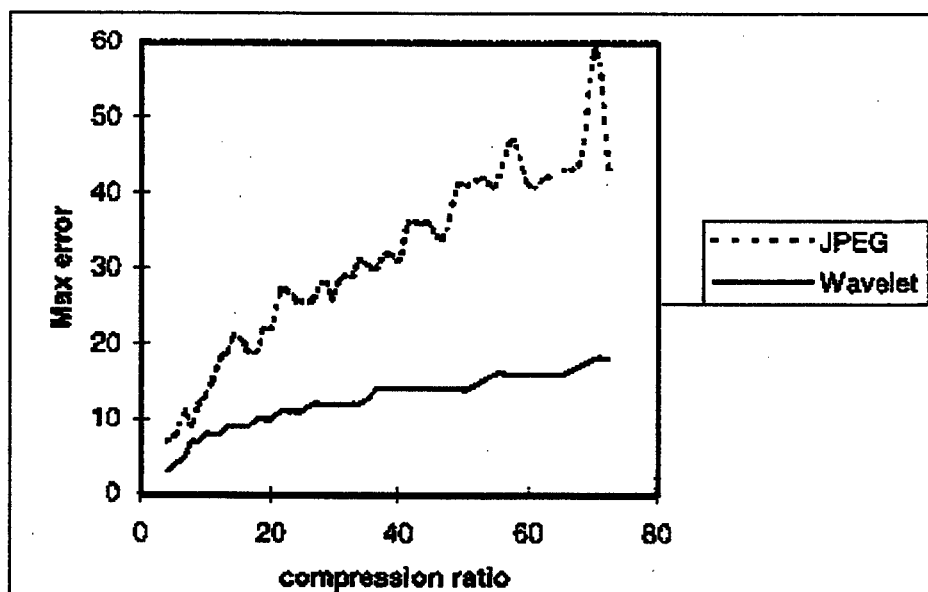


Figure 15 Max error

#### D. PURPOSE AND RATIONALE

Lossy compression algorithms significantly reduce the transmission times and storage space required for digital imagery. This reduction of image file size is necessary to meet increasing imagery requirements without upgrading current systems throughout



the military. Additionally, the military does not have a standard format for tactical imagery. The standardization of the image format will allow for seamless transfers of imagery during joint operations. Currently, N6 is evaluating these three lossy algorithms ICE, LBR, and RTN, to replace the current algorithm being used by the Navy. All three of these new algorithms can achieve compression ratios in excess of 60 times the maximum compression ratio of the algorithm currently used by the Navy. The Navy has proprietary rights to the code for RTN; therefore, selecting either ICE or LBR will require additional funding. This thesis will help N6 to determine if RTN should be selected as the Navy's new compression algorithm, or ultimately the DoD's.

Ultimately, this thesis will provide information to the DoD for procuring image compression software for the 21<sup>st</sup> century. Specifically, the thesis will compare the three lossy algorithms LBR, ICE, and RTN to the current compression standard currently used by the DoD. Finally, if ICE or LBR are judged better than RTN, determine if they are significantly better than RTN.

## **VI. METHODS**

### **A. GENERAL METHODS**

Four experiments are conducted to compare the performance of three algorithms. Reaction time and accuracy is collected for target detection and identification testing using both simple and complex background images. Additionally, pairwise subjective comparisons of image quality are collected.

### **B. DETECTION**

#### **1. Participants**

Five volunteer subjects for this experiment, consisted of three men and two women. All possess at least 20/20 corrected vision. The average subject age is 31 with a standard deviation of three. Subjects are naive to the purpose of the experiment and none have participated in previous visual search experiments.

#### **2. Apparatus**

The experimental workstation consists of a Pentium 200 MHz personal computer equipped with a Texas Instruments TMS340 Video Board and the corresponding TIGA Interface to Vision Research Graphics (VRG) software. The stimuli are presented on an IDEK MF-8521 High Resolution color monitor (21" X 20" viewable area) equipped with an anti-reflection, non-glare, P-22 short persistence CRT. Pixel size is .26' horizontal by .28' vertical, 800 X 600 square pixel resolution and the frame rate is 98.9 Hz. Brightness of the monitor is linearized by means of an 8-bit look-up table (LUT) for the red, blue, and green guns. Responses are recorded on the number pad of a standard computer

keyboard. The monitor and keyboard are placed on separate desks with a black cloth draped over both to prevent surface glare. Mesopic viewing conditions are maintained using a small floor lamp ( $6.8 \text{ cd/m}^2$  luminance) placed on the floor behind the IDEK monitor. A chair and a chin rest (both adjustable) are provided for subject comfort and to help maintain the appropriate distance and viewing angle.

### **3. Stimuli**

The images consist of 10 background scenes of rural and urban settings, with a target located in one of three regions (center, right, or left). The distracter images use the same background scenes, but with no target. Each of the images are compressed by the Applied Physics Laboratory's image coding division, utilizing RTN and LBR, at five image qualities. The target is a man standing or sitting in plain view. The images are then cropped to a square 460 X 460 pixel size in order to simulate output devices commonly found in military applications. The net result of this process is 600 images, 300 images with targets (10 scenes x 3 target locations x 5 compression ratios x 2 algorithms) and 300 distracter images.

After manipulation, all stimuli are converted to 8-bit, indexed color, IBM compatible image files for interface with the experimental hardware and software. The mean luminance of the images presented is  $5.7 \text{ cd/m}^2$ . Due to the test equipment limitation of 256 colors in PCX format, the images are converted from the 24bit-gray scale to 8bit-gray scale. Image Alchemy is used to do this using a Floyd-Steinberg dithering process. Due to limitations in the LUT of the Vision VRG Software, "noise" is introduced in the upper regions of some of the images that are compressed to 125% of

their original size. This anomaly does not significantly influence the experiment, since the effected region does not contain the target.

#### **4. Procedure**

Subject's complete three sessions with short rest intervals between sessions. Each subject is read task instructions and given an opportunity to ask questions. Because there are only five subjects, a "randomized block" design is employed where the subjects are the blocking variables and images are shown in a random order to control for nuisance variables such as learning, fatigue etc. Blocking reduces variability due to subjects' individual differences so that potential differences in the sensory and scene differences can be discerned. (Hayes, 1988)

In vision research, there are 'targets,' which are the objects of interest, or 'distracters,' which are everything else. For this experiment, images containing a signal are considered targets and the images where a signal is not present are considered distracters. A standard visual search paradigm requires that equal numbers of targets be presented in an experiment. Accordingly, one matching distracter image for each scene is provided.

Stimuli are flashed (using a square wave pulse) on the center of the screen in a 10 cm X 10 cm square and are viewed from a distance of 148 cm, thus subtending a  $5.6^\circ$  x  $5.6^\circ$  visual area on the retina. The stimulus is present until the subject makes a selection or until a maximum of six seconds viewing time has elapsed. The experiment then proceeds to the next trial, 200 ms after the response is made. A tone provides feedback

when the subject responds incorrectly for the type of image (target/distracter) that is presented.

## **C. ACCURACY IN IDENTIFICATION TEST**

### **1. Subjects**

This test is divided into two separate tests, simple and complex. The division of this test is covered in the stimuli section.

#### ***a. Simple***

The 26 subjects participating in the study are all U.S. Navy active duty. Twenty-four of the subjects are enlisted with an average rank between E-3 and E-4. The average length of service completed is 4.2 years. Five of the enlisted are female. The two officers tested have completed a Department head tour and are both Lieutenant Commanders with an average length of service of 14.5 years. All subjects have correctable 20/20 vision in both eyes.

#### ***b. Complex***

This experiment uses Ten subjects, seven male and three females. All subjects have correctable 20/20 vision in both eyes.

### **2. Apparatus**

#### ***a. Simple***

The test computers all have 90Mhz Pentium CPUs, with 16Mbits memory or better. A 15 inch-color video monitor with .28 dot pitch resolution running at 800 X 600 display size is used. The test is given at several locations using different machines. The user is seated approximately two feet in front of the monitor. The exact distance and

monitor are not controlled, which may add to the variations in the response. Because of the varied equipment in use today by DoD, no standard display is chosen for this experiment. A Visual Basic program was written to display images randomly while recording the subjects' accuracy and response time. The images are centered on the screen, and the time required to identify the target is recorded in 100 ms intervals.

***b. Complex***

The complex image test uses a single Pentium II 233 computer with a 21" NEC MultiSync XE21 monitor. The monitor resolution is set to 1024 X 768 pixels. All other aspects of the experiment are the same as the simple image accuracy test.

**3. Stimuli**

This test is further divided into the identification of both an object with a simple background, and an object with a complex background. These two tests are referred to as the simple images and complex images, respectively. The simple images are composed of U.S. Navy ships, both on the open sea and near land. There are seven different types of ships. Each image is compressed with RTN, LBR, and ICE at five image qualities. Several images are not compressed to every image quality level due to software limitations. All the scenes are 800 X 600 pixels in size. The net result of the compressions is 377 images (7 ships x 4 views x 3 algorithms x 5 image qualities + 28 original images - 71 unattainable images).

The complex images are composed of automobiles. There are five different types of cars, and four different views of each car. Each image is compressed with RTN, LBR, and ICE at five image qualities. Several images are not compressed to every image

quality level due to software limitations. All the scenes are 640 X 480 pixels in size. The net result of the compressions is 300 images (5 cars x 4 views x 3 algorithms x 5 images).

Each original image is compressed using the three new compression algorithms at five compression ratios. All combinations of algorithm and compression ratios are applied to each image to produce fifteen new images. The LBR compression algorithm is used first on each image. The LBR is the most limiting of the three algorithms, because it provides little control of compression ratios. Inputting an image quality level into LBR and RTN indirectly controls the compression ratio of the final image. LBR has only five compression qualities; on the other hand, RTN has one hundred. ICE has both an image-quality setting and image-compression-ratio setting. ICE can compress images from 2 to one, to 100 to 1. The compression ratio is calculated by dividing the original file storage size by the storage of the image at each compression quality. The compression ratio is used to verify that the final compressed images are of equivalent compression. Compressed images are considered equivalent in image quality if their compression ratio is within 10 to 1 of each other.

RTN is applied to the same images that are compressed with LBR. The mean compression ratios at each of the five image qualities are calculated. ICE is set to the mean compression ratio for each image. Due to ICE being limited to a 100 to 1 compression ratio, only the mean compression ratios of less than 110 to 1 are compressed with ICE.

#### **4. Procedure**

The accuracy test is designed to determine the effect each algorithm has on image quality. In addition, how the increased compression ratios affect the ability of subjects to identify objects in the images is measured. Each subject is shown an image and asked to identify the item depicted. The image remains on the screen until the subjects make a mouse click on the image. The subject is then presented a list of choices from which the subject is asked to indicate the object that is displayed. The answer is recorded along with the image viewed. Each subject sees each image in the data set. The images are randomized each time by the computer to reduce the possibility of either a learned response or an order effect. A blank screen is displayed for 500 ms before displaying the next image.

#### **D. REACTION TIME IN IDENTIFICATION TEST**

##### **1. Subjects**

The subjects that participate in the complex image accuracy test also participated in the complex image reaction time test. Likewise, the subjects that participated in the simple accuracy test also participate in the simple image reaction time test.

##### **2. Apparatus**

The apparatus for the complex image accuracy test is used in the complex image reaction time test. Likewise, the apparatus for the simple accuracy test is used by the simple image reaction time test.



### **3. Stimuli**

The stimulus for the complex image accuracy test is used in the complex image reaction time test. Similarly, the stimulus for the simple accuracy test is used by the simple image reaction time test.

### **4. Procedure**

The reaction time experiment is run concurrently with the accuracy test. During the accuracy test, the program records the reaction time of the subject. The reaction time is calculated from the time the image is displayed to the time the subject clicks on the image with the mouse. The reaction time is recorded in 100 ms increments.

## **E. PAIRED COMPARISON**

### **1. Subjects**

#### ***a. Simple***

Twenty-five subjects, 24 active-duty U.S. Navy personnel and one Marine, participate in this portion of the study. All of the subjects are enlisted with an average rank between E-3 and E-4. The average length of service completed is 4.0 years. Five of the enlisted are female. All subjects have correctable 20/20 vision in both eyes.

#### ***b. Complex***

Nine subjects, seven male and two females, participate in this experiment. Eight of the nine subjects are military officers with an average length of service of eight years. The eight officers are either of pay grades O-3 or O-4. The remaining subject is civilian. All subjects had correctable 20/20 vision in both eyes.

## **2. Apparatus**

The apparatus for the complex image accuracy test is used in the complex image reaction time test. Similarly, the apparatus for the simple accuracy test is used by the simple image reaction time test.

## **3. Stimuli**

The stimulus for the complex image accuracy test is used in the complex image reaction time test. Likewise, the stimulus for the simple accuracy test is used by the simple image reaction time test. The simple test has additional images added to increase the number of images compressed at lower image quality levels for ICE. The additional images are of the same type as the original set. Sets of image pairs are made from the compressed images. Each pair is of the same scene at the same compression level. Every combination of algorithms is used.

## **4. Procedure**

The subjects complete two sessions with a short rest interval between sessions. The objective of this experiment is to collect a more subjective ranking of the three algorithms. A Visual Basic program displays each image in an image set centered on the screen for 500 ms in a random order. The screen is blanked for 500 ms between the image pairs. The subject is then given the following choices: the first image is better, the second image is better; or the images are the same. The image sets are shown in both orders of presentation to reduce the effect of an order effect on the outcome.



## **VII. DATA ANALYSIS**

LBR is limited to five preset image qualities, thus it is not possible to compress each scene to the same compression ratio. For this reason, most of the data analysis is based on the LBR image quality settings. Compressed images are considered equivalent in image quality if their compression ratio is within 10 to 1. The difference in compression ratios is minimized to reduce any bias towards an algorithm. This difference is only a factor in image quality levels one and two; image quality levels three, four, and five have compression ratio differences of less than 2 to 1.

Three independent experiments are conducted. The first experiment collects accuracy and reaction time to determine if a target is in the scene. This experiment is an initial trial to determine if further testing is warranted. The second experiment collects accuracy and reaction time to determine target identification. The final experiment collects the subjects' subjective preference between pairs of images.

### **A. DETECTION**

ICE is not available for the detection experiment, therefore only RTN and LBR are evaluated.

#### **1. Accuracy**

A 2 x 5 x 5 x 2 Analysis of Variance (ANOVA) is conducted, where the four factors are the type of algorithm (LBR or RTN), the compression ratio (1, 2, 3, 4, 5), the identity of the subject (A, B, C, D, E) and the target (target or distracter). The dependent variable of the ANOVA is the mean proportion correct of each object type. Stepwise

linear regression is used to arrive at final ANOVA model. This model has been checked to verify that all significant interactions are included in the model. The residuals are also checked to verify the ANOVA modeling assumptions.

The residual values show no trend and equal variance. With the exception of the tails, the residuals also appear normally distributed. With the large sample size in this experiment, this departure from normality will not effect the interpretation of the ANOVA results. As can be seen in Table 8, all four factors, subject, algorithm, compression ratio and target are significant. In addition there appears to be important two way and three way interactions. A significant main effect for algorithm shows that the subjects have fewer errors in identifying targets with the RTN compared to LBR (Figure 16). Compression main effect shows that as the image quality decreases (compression increasing), the accuracy of identifying targets decreases. The subject main effect shows the variability in the ability of subjects to identify targets correctly. The type of image, target or distracter, is the most significant main effect. The subjects' ability to identify images correctly is significantly lower for identifying targets than for identifying distracters. There are no non-significant main effects.

	Df	Sum of Sq	Mean Sq	F Value	Pr(F)
subject	4	0.328267	0.082067	12.0211	0.000000128
algorithm (a)	1	0.080278	0.080278	11.7590	0.000981235
compression (c)	4	0.455933	0.113983	16.6962	0.000000001
target (t)	1	2.160900	2.160900	316.5272	0.000000000
c and t	4	0.399044	0.099761	14.6129	0.000000007
c and a	4	0.115222	0.028806	4.2194	0.003874413
a and t	1	0.096100	0.096100	14.0767	0.000340917
t and a and c	4	0.118511	0.029628	4.3399	0.003247522
Residuals	76	0.518844	0.006827		
Residual standard error: 0.08262506					

**Table 8 ANOVA of Accuracy of Detection**

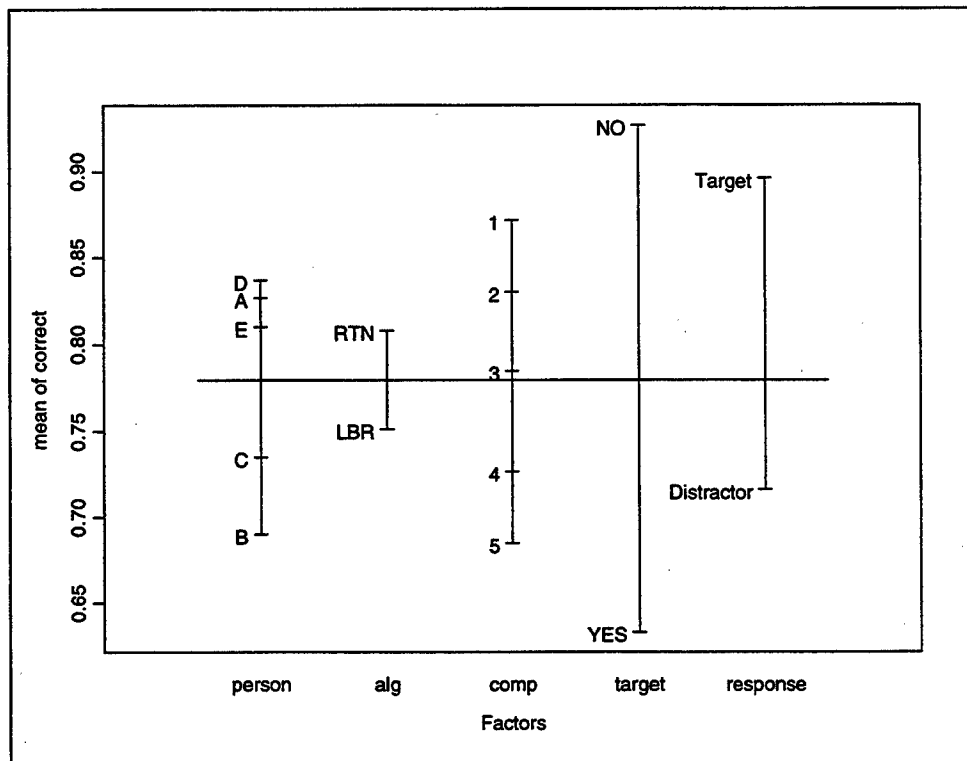


**Figure 16 Proportion Correct by Each Factor, Detection**

The factors combine with each other in two-way interactions to affect the accuracy of identifying targets. A compression by target interaction shows that as the compression ratio increases (lower image quality), the subjects identify distracters more accurately than targets (Figure 17). The compression by algorithm interaction shows a more rapid decrease in accuracy as image quality decreased for LBR compared to RTN (Figure 18). The algorithm by target comparison interaction shows a significant difference, in that images compressed with RTN are identified more accurately than images compressed with LBR (Figure 19). RTN and LBR do not affect the distracters. The effect of the algorithm is expected from the results of the interactions of the image quality and target type with the algorithm.

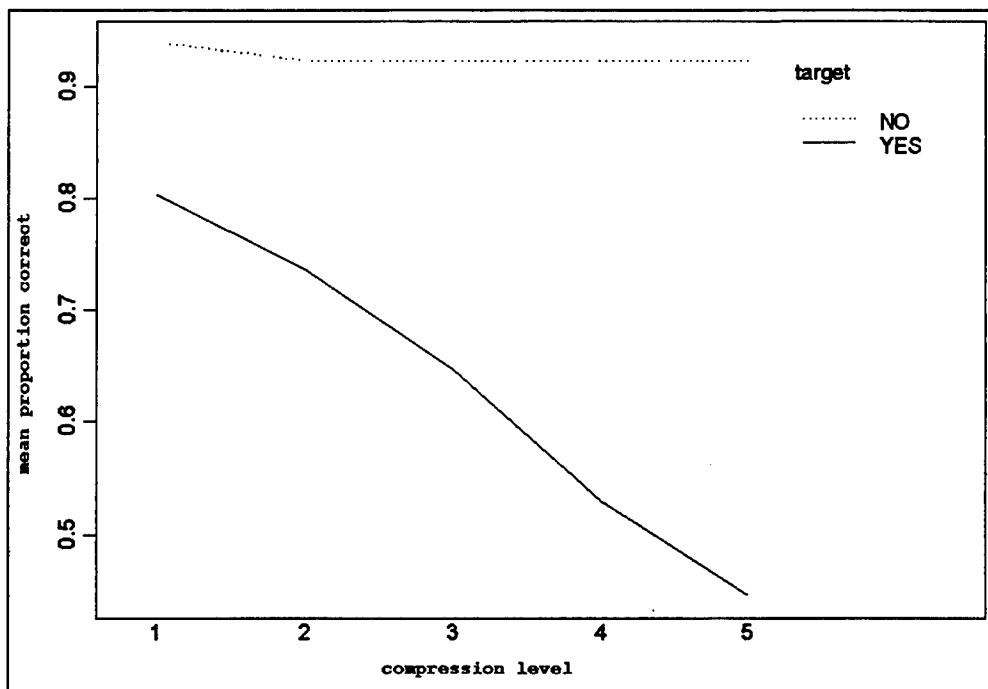


**Figure 17 Proportion Correct by Compression Level and Target, Detection**

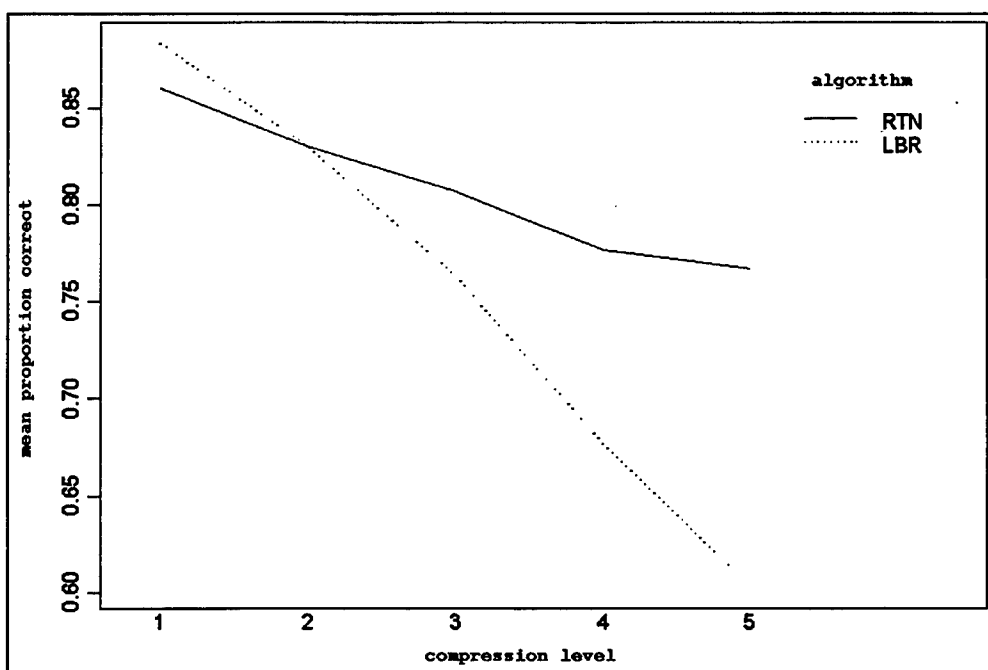


**Figure 18 Proportion Correct by Compression Level and Algorithm, Detection**

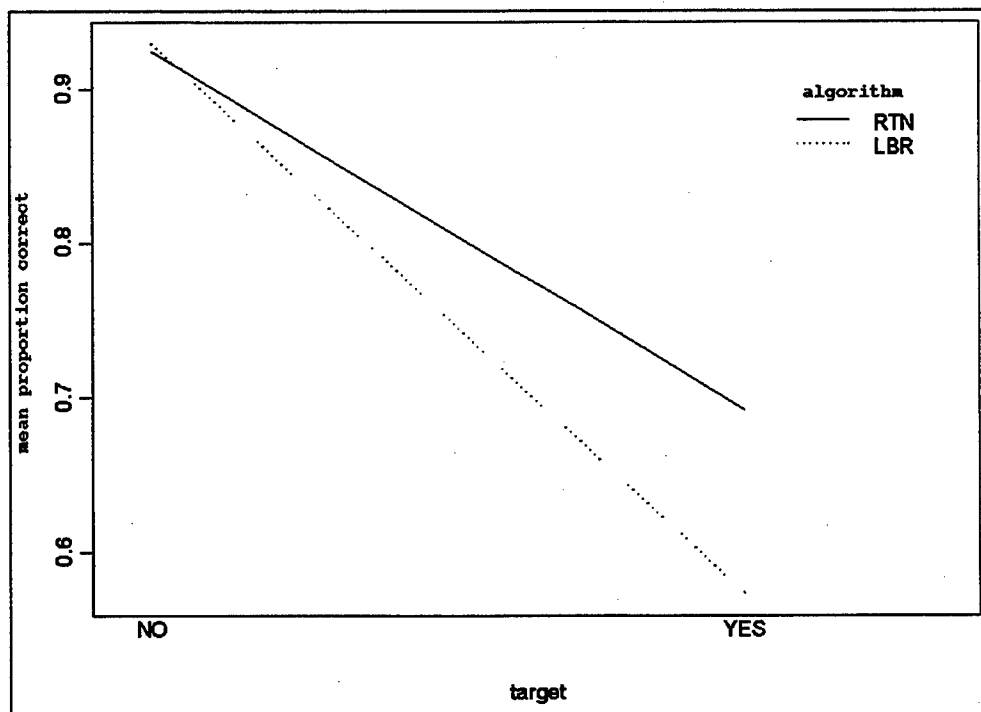


**Figure 19 Proportion Correct by Target and Algorithm, Detection**

The three-way interaction of target and algorithm with compression is significant. The plot of this three-way interaction (Figure 20) shows the different effects of target and algorithm have on accuracy as compression increases. There is no difference in the distracter at any compression ratio. However, the target algorithm lines show there is a difference as the compression ratio increases. All other interactions are non-significant.



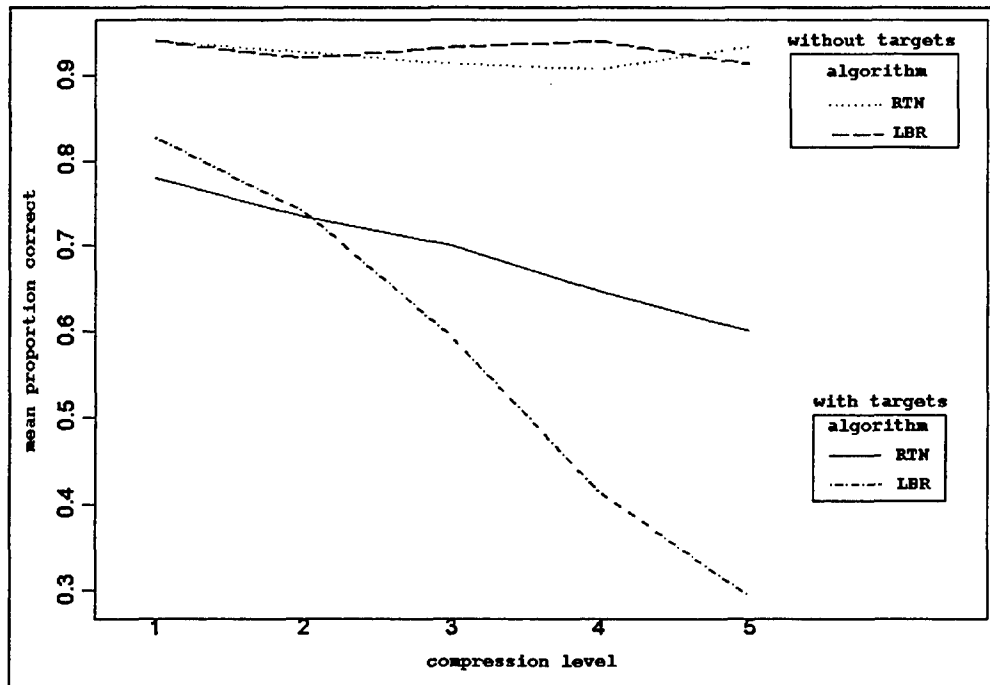


**Figure 20 Proportion Correct by Compression Level, Algorithm and Target, Detection**

## 2. Reaction Time

A  $2 \times 5 \times 5 \times 2$  ANOVA is calculated where the four factors are the type of algorithm (LBR or RTN), the compression ratio (1, 2, 3, 4, 5), the identity of the subject (A, B, C, D, E) and the target (target or distracter). The dependent variable of the ANOVA is the average reaction time for each object type. Stepwise linear regression was used to develop the model used in the ANOVA table. The final model has been checked to verify that all significant interactions are included in the model. The ANOVA results are shown in Table 9.

	Df	Sum of Sq	Mean Sq	F Value	Pr(F)
subject	4	6231644	1557911	53.0125	0.0000000
algorithm(a)	1	175592	175592	5.9750	0.0166014
compression level(c)	4	22237	5559	0.1892	0.9434430
target(t)	1	3227137	3227137	109.8129	0.0000000
c and t	4	717475	179369	6.1036	0.0002320
a and t	1	199300	199300	6.7818	0.0108884
Residuals	84	2468559	29388		
Residual standard error: 171.4281					

**Table 9 ANOVA of Reaction Time of Detection**

ANOVA requirements of equal variance and normality of the residuals are again verified. The residual values show no trend and equal variance, with the exception of the tails, the residuals appear normally distributed. Subjects took longer to identify targets with RTN, than with LBR (Figure 21). The effect of the subjects shows the variability in reaction time of subjects to correctly identify targets. The image type affects the subjects' reaction time in identifying images. The distracters take significantly longer to identify than targets.

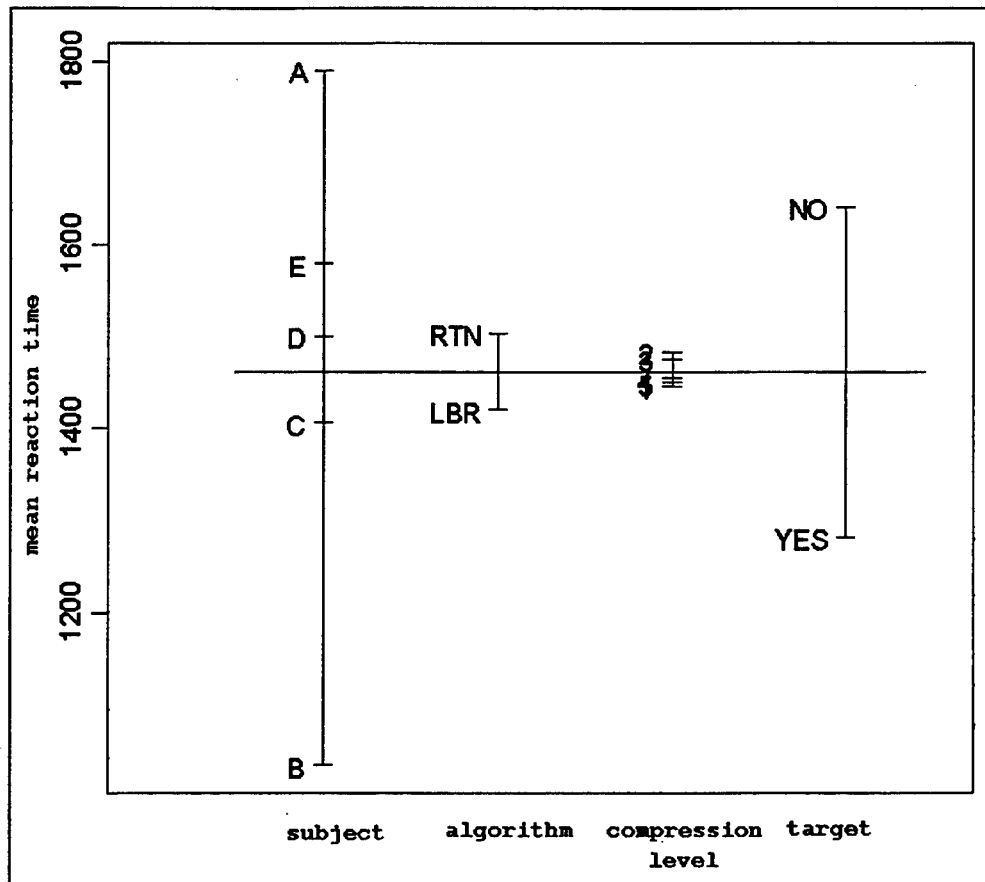


**Figure 21 Mean Reaction Time by Each Factor, Detection**

The mean reaction times differed by less than 25 milliseconds from the slowest to the fastest compression ratio (Figure 21). This gives the impression that differences in compression levels do not effect mean reaction times. However, a significant compression by target interaction can be seen (Figure 22). The subjects' reaction time decreases as the compression ratio increases for identifying distracters. Similarly, the reaction time increases when identifying targets as the compression ratio increases. The algorithm-by-target comparison also shows a significant difference. The reaction time increases for RTN compressed images compared to LBR. The reaction time for identifying distracters is unchanged by both algorithms (Figure 23).

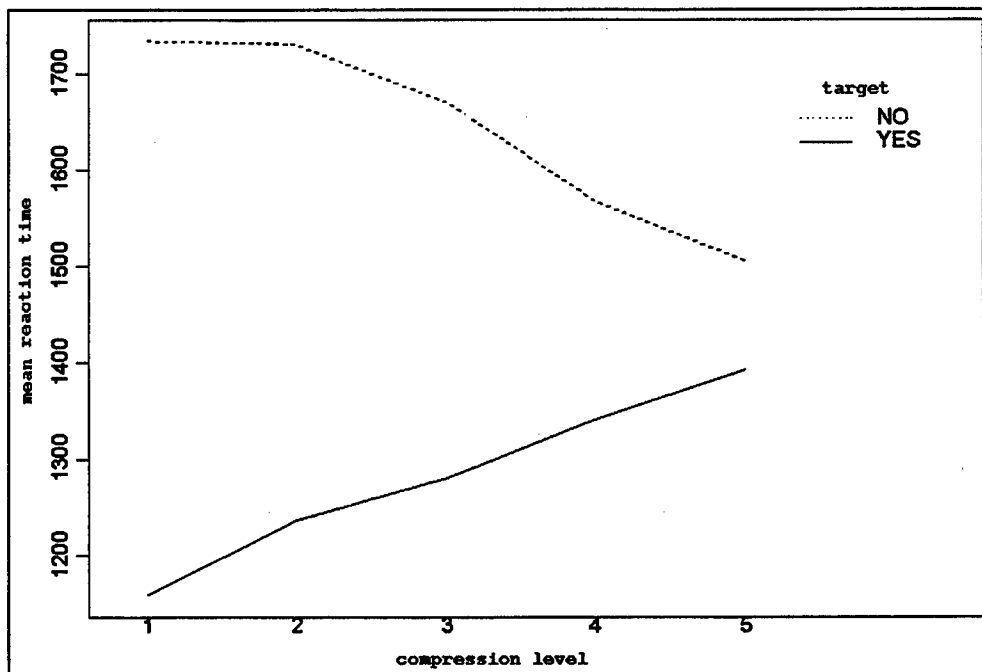


**Figure 22 Mean Reaction Time by Compression Level and Target, Detection**

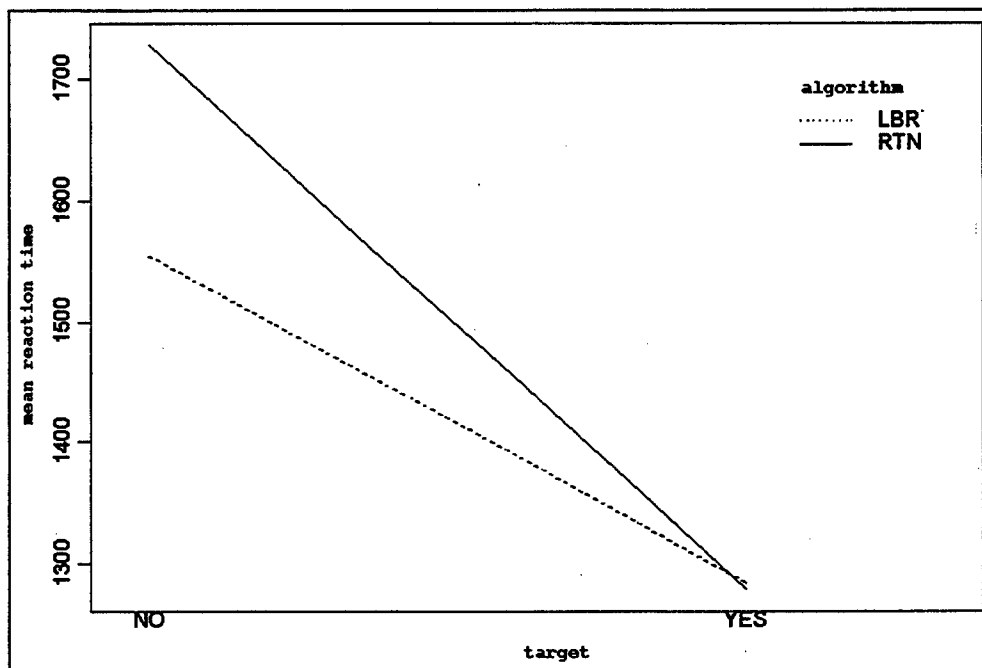


**Figure 23 Mean Reaction Time by Target and Algorithm, Detection**

None of the three-way interactions are significant.

## B. ACCURACY IN IDENTIFICATION TEST

### 3. Simple Images

Due to ICE being limited to a maximum compression ratio of 100 to 1, all three algorithms are only compared at image compression settings four and five. The level of accurately identifying ICE images is not considered at image compression level three due to having only two observations per subject. A stepwise regression is used to develop the initial model for the one-way ANOVA. The initial model is then modified to reflect significant interaction terms.

A 4 x 5 x 26 x 8 ANOVA is calculated where the four factors are the type of algorithm (LBR, RTN, ICE and ORG), the image quality (1, 2, 3, 4, 5), the identity of the subject (unique number) and the target (0, 2, 3, 4, 5, 6, 8, 9). The dependent variable of the ANOVA is the proportion correct of each object type. The final model was checked to verify that all significant interactions are included in the model. The ANOVA results are shown in Table 10.

	Df	Sum of Sq	Mean Sq	F Value	Pr(F)
Subject(s)	25	138.3402	5.53361	177.1485	0.00000000
algorithm(a)	3	0.9664	0.32214	10.3128	0.00000096
image quality(q)	4	2.1325	0.53313	17.0671	0.00000000
object(o)	7	128.6137	18.37338	588.1904	0.00000000
s and q	125	4.7854	0.03828	1.2256	0.04899388
s and o	175	119.6062	0.68346	21.8799	0.00000000
o and a	21	1.1331	0.05396	1.7273	0.02106095
q and o	28	1.3580	0.04850	1.5526	0.03243134
Residuals	2393	74.7504	0.03124		
Residual standard error: 0.1767403					

**Table 10 ANOVA of Accuracy of Simple Images**

A significant effect by algorithm shows that there is a difference in the ability to identify objects when compressed with different algorithms. From the least effect on

accuracy to greatest reduction in accuracy, the algorithms are the original image, ICE, RTN, and LBR (Figure 24). The effect of compression levels shows that as the image quality decreases (compression increases) the accuracy of identifying objects decreases. The main effect of algorithm and image quality can be better seen in Figure 25. The effect of object shows that the type of ship has a major effect on accuracy. Subject interviews after the experiment reveal that several of the subjects could not identify amphibious ships. The subjects show a wide range of ability in identifying ships. This result is expected after having reviewed the post-experiment interviews. Over half of the subjects participating have no fleet experience and are in the beginning phase of their ship identification training.

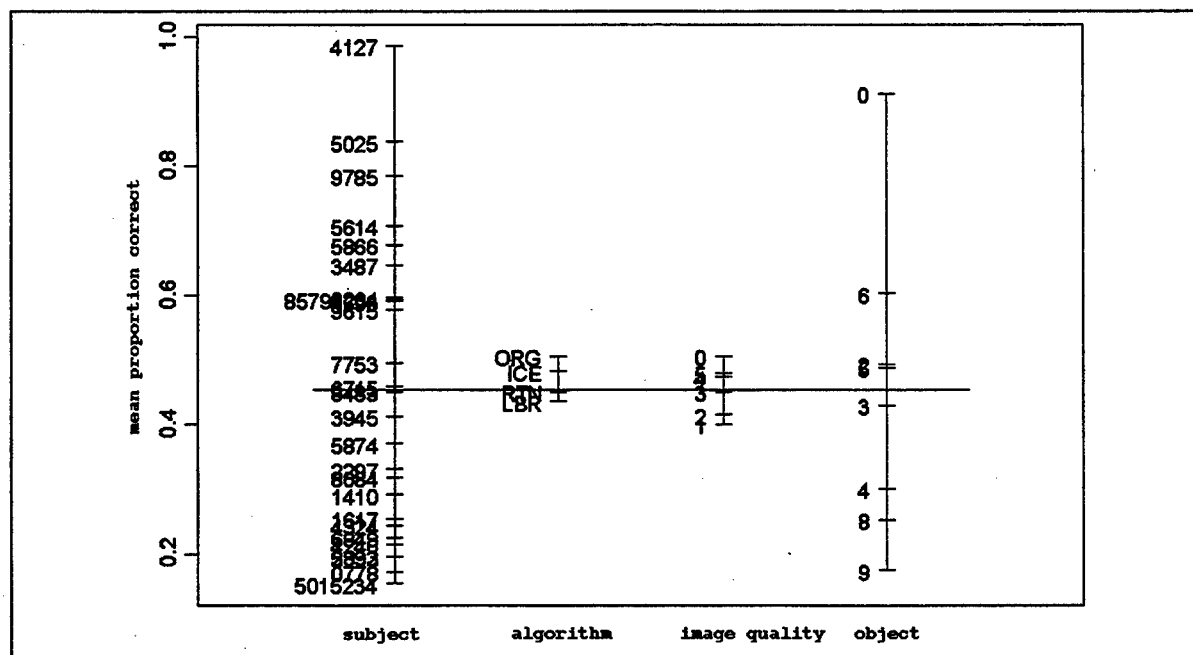
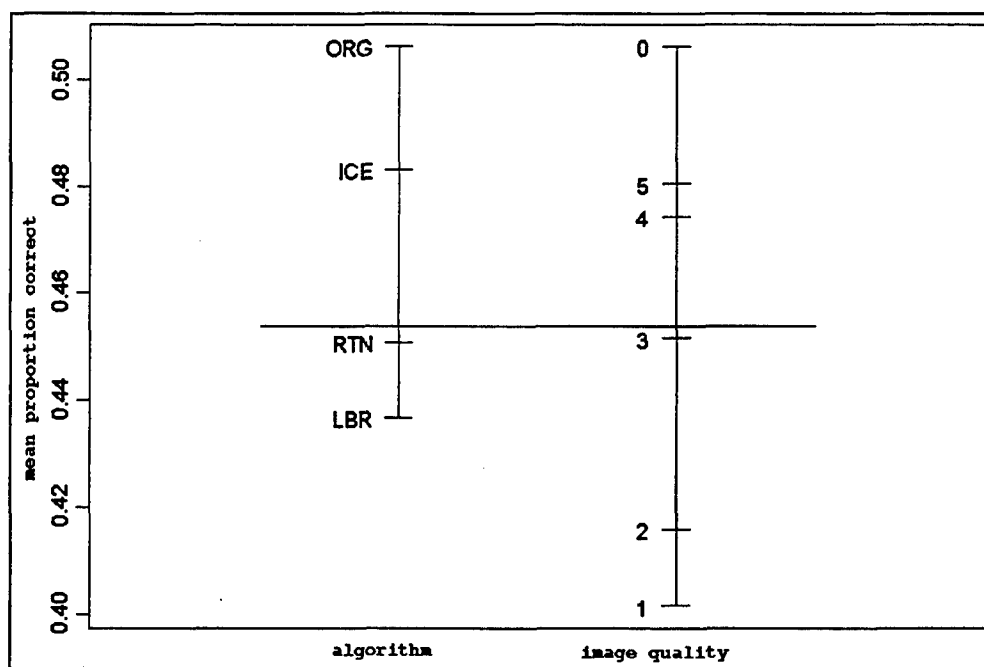


Figure 24 Proportion Correct by Factor, Simple Background



**Figure 25 Proportion Correct by Algorithm and Image Quality Factors, Simple Background**

Four of the six possible interactions between algorithm, image quality, subject, and object are significant. A significant algorithm by object interaction shows that the compression algorithm affects the accuracy of identifying objects depending on the object type (Figure 26). The image quality by object interaction shows that not all objects compress equally (Figure 27). The varied level of image compression affects the subjects' accuracy in identifying the objects. The general trend is that the uncompressed images are identified with the highest accuracy. The most compressed images (lowest image quality) have the lowest identification rate. This general decrease is expected.

Additionally, the addition of the uncompressed images shows that the algorithms used to compress the images are not solely responsible for the subjects' inability to identify the ships. A significant subject-object interaction shows that there is a wide range of ability in identifying different target types by the subjects. This large difference

is attributed to the disparity between the experienced and non-experienced subjects discussed under main effects. The graph shows no obvious trends and is therefore not included.

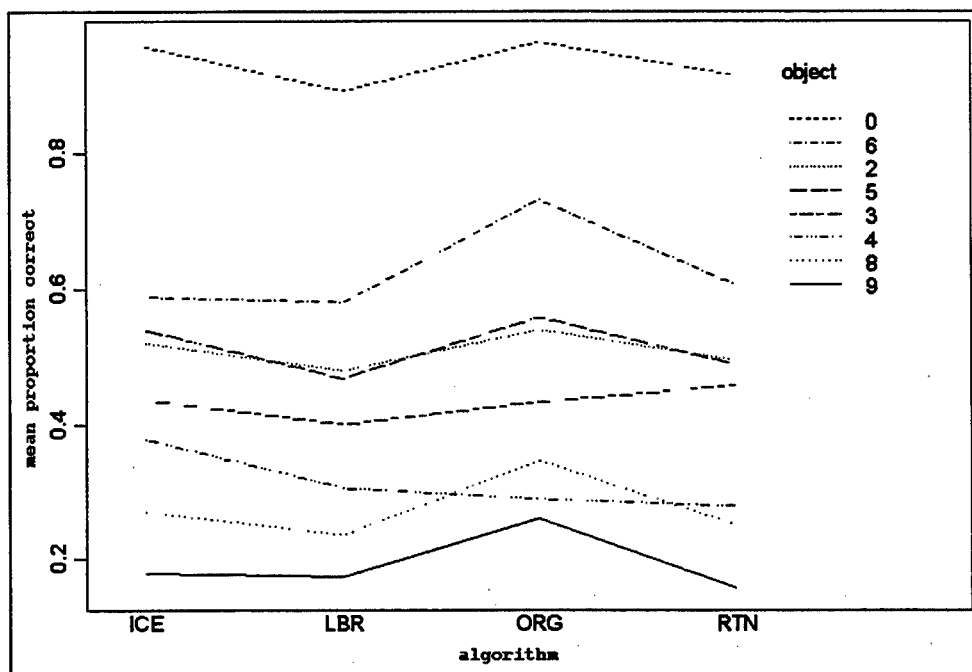
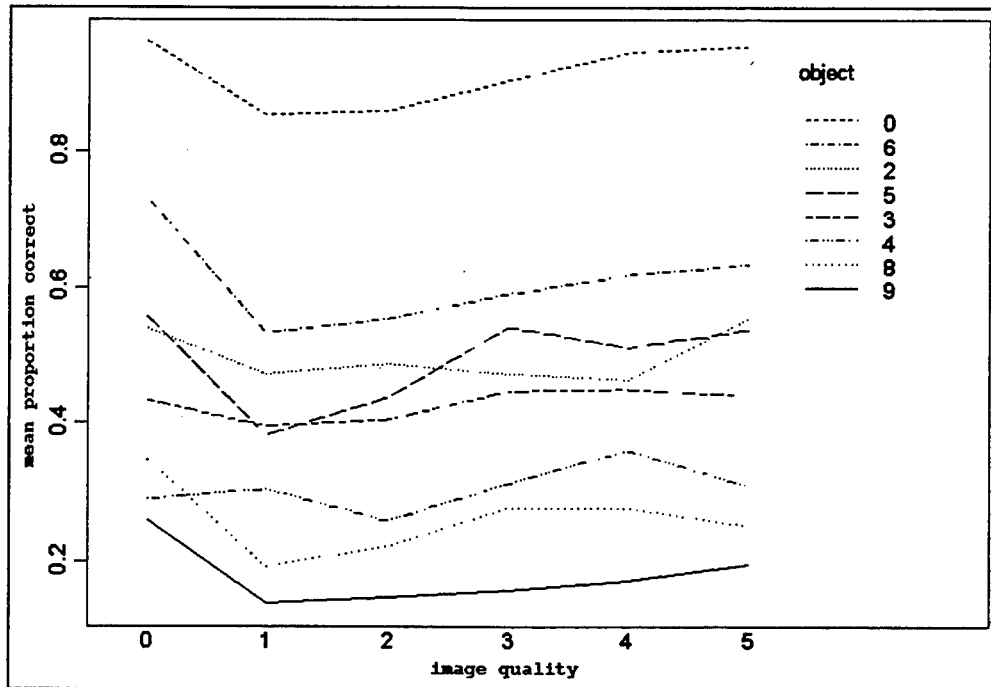


Figure 26 Proportion Correct by Algorithm and Object, Simple Background





**Figure 27 Proportion Correct by Image Quality and Object, Simple Background**

There is no a significant interaction between the compression algorithm and the compression ratio (image quality), but the algorithms did affect the accuracy. The differences in the interaction between algorithm and compression ratio are used to help determine which compression algorithm will be used in the future. The general trend is that images compressed with ICE are identified with greater accuracy for image qualities four and five (least compressed) (Figure 29). At image quality settings one through four, images compressed with RTN are more accurately identified than images compressed with LBR.

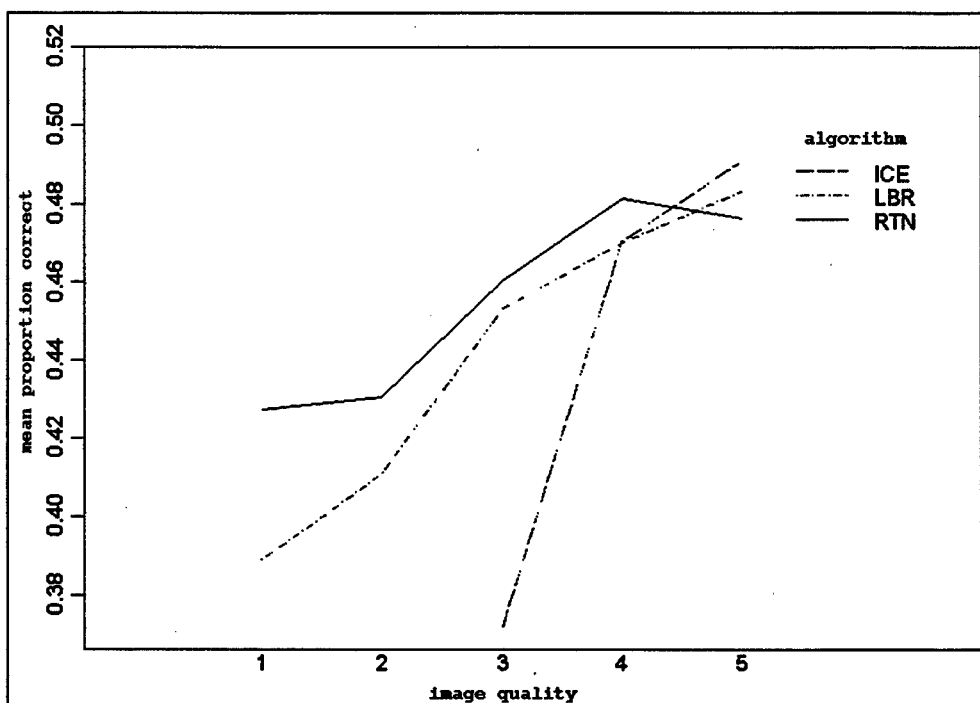


**Figure 28 Proportion Correct by Image Quality and Algorithm, Simple Background**

A pair comparison using Bonferroni's method was used to check for significance between RTN and ICE. Using a 0.01 level of significance ( $Z_{\frac{\alpha}{3}} = 2.7131$ ) there is significance only at image quality level three (Table 11). A 0.05 level of significance ( $Z_{\frac{\alpha}{3}} = 3.1280$ ) does not alter the results of the paired comparison.

image quality level	test stat
3	3.7805
4	0.6334
5	0.8322

**Table 11 Test Statistics for Paired Test of Accuracy**

### 1. Complex Images

Due to the image complexity, the maximum compression ratio achieved by all the algorithms is greatly reduced compared to the simple images. ICE's limitation of a maximum compression ratio of 100 to 1 allowed for testing all three algorithms down to

image quality two. Again only RTN and LBR are compared at the lowest image quality (1), the highest compression ratio. A stepwise regression is used to develop the initial model for the one-way ANOVA. The initial model is then modified to reflect significant interaction terms.

A 3 x 6 x 10 x 5 ANOVA is calculated where the four factors are the type of algorithm (LBR, RTN, and ICE), the image quality (1, 2, 3, 4, 5, 6), the identity of the subject (unique number) and the target (SU, SE, MV, SP, ST). The dependent variable of the ANOVA is the proportion correct of each object type. The final model has been checked to verify that all significant interactions are included in the model. The ANOVA results are shown in Table 12.

	Df	Sum of Sq	Mean Sq	F Value	Pr(F)
Subject(s)	9	0.713889	0.079321	6.24810	0.00000002460
Algorithm(a)	2	0.278208	0.139104	10.95721	0.00002257274
image quality(q)	5	1.315718	0.263144	20.72778	0.00000000000
object(o)	4	4.333594	1.083398	85.33911	0.00000000000
a and q	8	1.044823	0.130603	10.28757	0.00000000000
s and o	36	3.545399	0.098483	7.75751	0.00000000000
a and o	8	0.440351	0.055044	4.33579	0.00004729296
q and o	20	0.722596	0.036130	2.84594	0.00004625443
q and o and a	32	0.975126	0.030473	2.40033	0.00004495935
s and o and q	225	4.538976	0.020173	1.58904	0.00001987130
Residuals	450	5.712847	0.012695		
Residual standard error: 0.112673					

**Table 12 ANOVA of Accuracy of Complex Images**

A significant effect of algorithm shows there is a difference in the subjects' ability to identify objects when compressed with different algorithms. From the least effect on accuracy to greatest reduction in accuracy, the algorithms are ICE, RTN, and LBR (Figure 29). The effect of compression levels shows that as the image quality decreases (compression increasing) the accuracy of identifying objects decreases. The image

quality level zero is formed from a set of RTN and ICE images.<sup>2</sup> Level zero images have an image quality between one and two. The effect of object shows that the object type had an effect on accuracy. The subject main effect shows that the subjects had an effect on accuracy. The subject effect on accuracy is less significant with the complex images due to the object selection for the test. To reduce the subject effect, easily identifiable cars are used as target objects. However, one of the cars is noticeably harder to identify (ST).

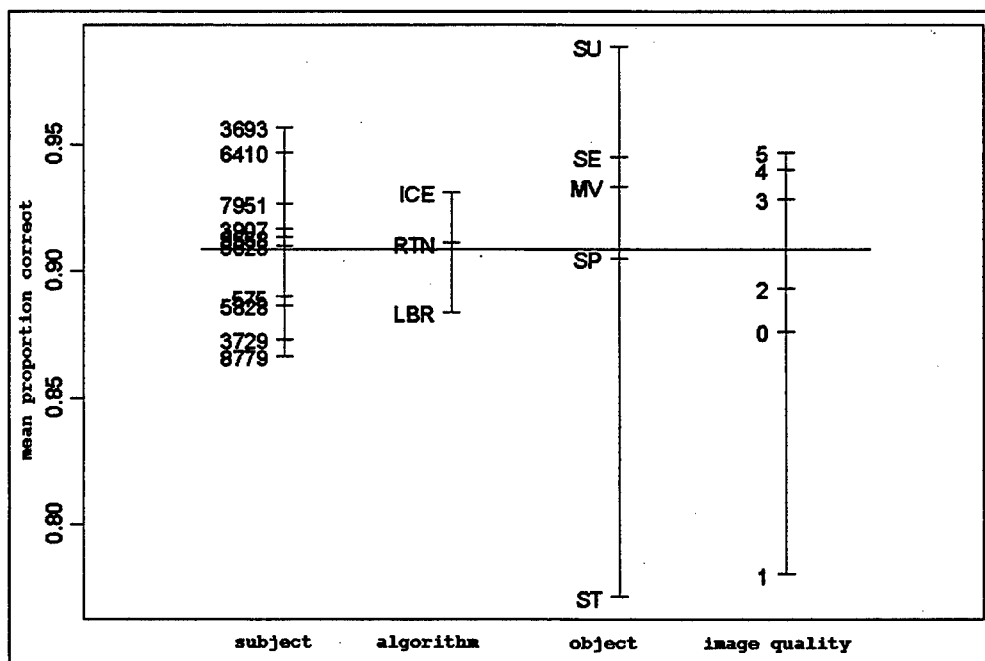


**Figure 29 Proportion Correct by Factor, Complex Background**

A significant algorithm by object interaction shows the effect of the object type on accuracy of identifying that type (Figure 30). The image quality by object interaction shows that not all objects compress equally (Figure 31). These varied levels of image compression effected the accuracy of the subjects in identifying the objects. The general

<sup>2</sup> These images would have been image quality one except that software limitations prevented the images from being compressed to the equivalent level of the LBR images.

trend is that the most compressed images (lowest image quality) have the lowest rate of identification. This general decrease is expected.

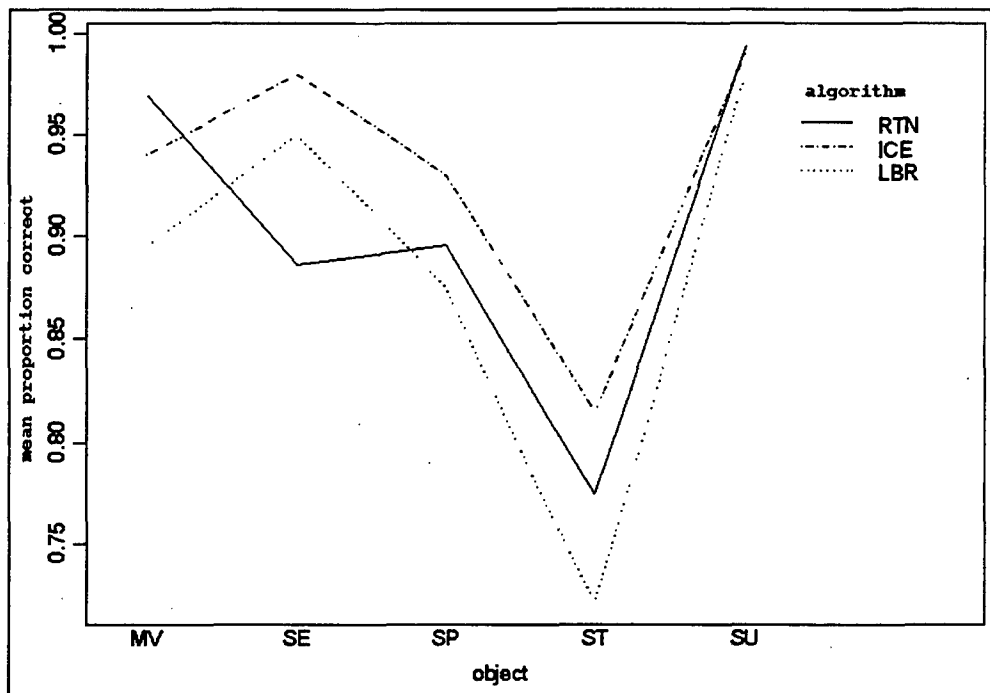


**Figure 30 Proportion Correct by Object and Algorithm, Complex Background**

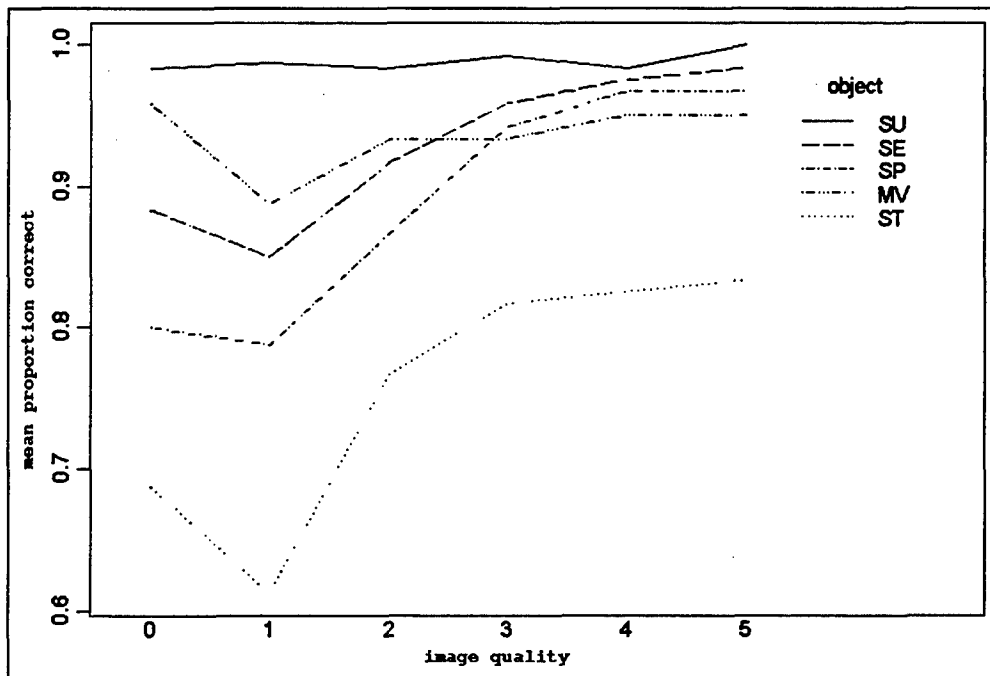


**Figure 31 Proportion Correct by Image Quality and Object, Complex Background**

A significant subject-object interaction shows that there is a significant differences among the subjects' abilities to identify different target types. The graph shows no obvious trends and is therefore not included. A significant interaction between the compression algorithm and the image quality shows that as image quality decreases (compression ratio increasing) accuracy also decreases (Figure 32). No discernable trends are evident in the remaining interaction terms and are not shown. A paired comparison gives a test statistic less then 1.6 at all levels between RTN and ICE. The critical Z value is 2.8070 at a 0.01 level of significance and 2.2414 at a 0.05 level of significance.

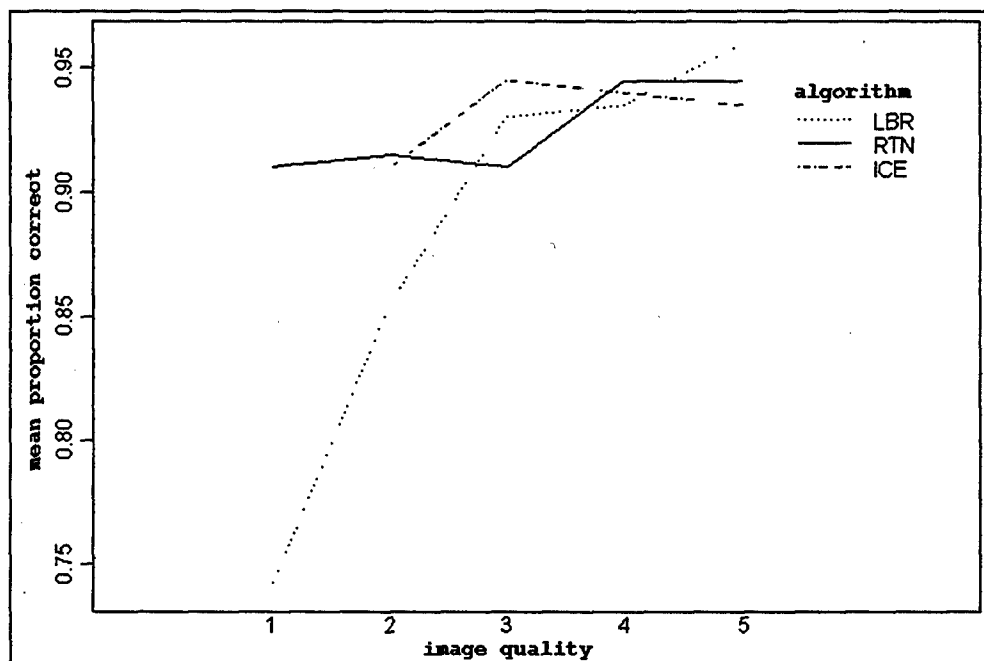


**Figure 32 Proportion Correct by Image Quality and Algorithm, Complex Background**

A linear regression is calculated for each algorithm against compression ratio (Figure 33). The regression shows that at compression ratios greater than 48 to 1 the subjects prefer ICE to RTN. Additionally, the subjects prefer RTN to LBR. The order of

preference is reversed at compression ratios less than 48 to 1. One of the images compressed with ICE is missed more often at the lower compression ratio than the higher compression ratio. The most likely reason is that there was a learning effect. However, the images are shown in a random order to reduce the learning effect.

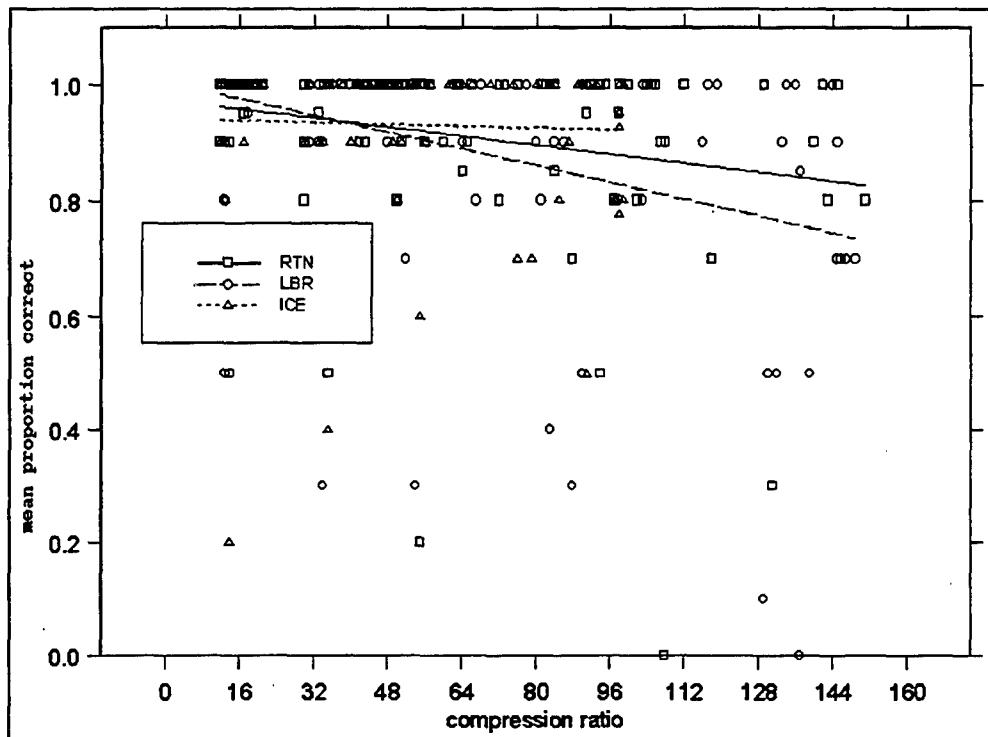


Figure 33 Linear Regression of Compression Ratio on Accuracy, Complex Images

## C. REACTION TIME IN IDENTIFICATION TEST

### 1. Simple Images

A 3 x 26 x 8 ANOVA is conducted where the four factors are the type of algorithm (ORG, LBR, RTN, and ICE), the identity of the subject (unique number) and the target (0, 2, 3, 4, 5, 6, 8, 9). The dependent variable of the ANOVA is the average reaction time for each object type. The final model was checked to verify that all

significant interactions are included in the model. The ANOVA results are shown in Table 13.

	Df	Sum of Sq	Mean Sq	F Value	Pr (F)
Subject(s)	25	1005.88	40.23500	6.812684	0.0000000
Algorithm(a)	3	26.68	8.89292	1.505770	0.2110333
Object(o)	7	187.49	26.78407	4.535141	0.0000486
S and a	75	651.82	8.69087	1.471559	0.0057007
S and o	175	1328.19	7.58967	1.285100	0.0085668
Residuals	2496	14741.12	5.90590		
Residual standard error: 2.430205					

**Table 13 ANOVA of Reaction Time of Simple Images**

A significant effect for subject shows that there is a difference in subjects' reaction time (Figure 34). This difference in subject ability is discussed in Chapter VII section B sub-section 2. The effect of object shows that the type of ship had a large effect on reaction time. Both algorithm and compression ratio (image quality) are non-significant main effects. However, algorithm is left in because of significant interaction terms involving algorithm.

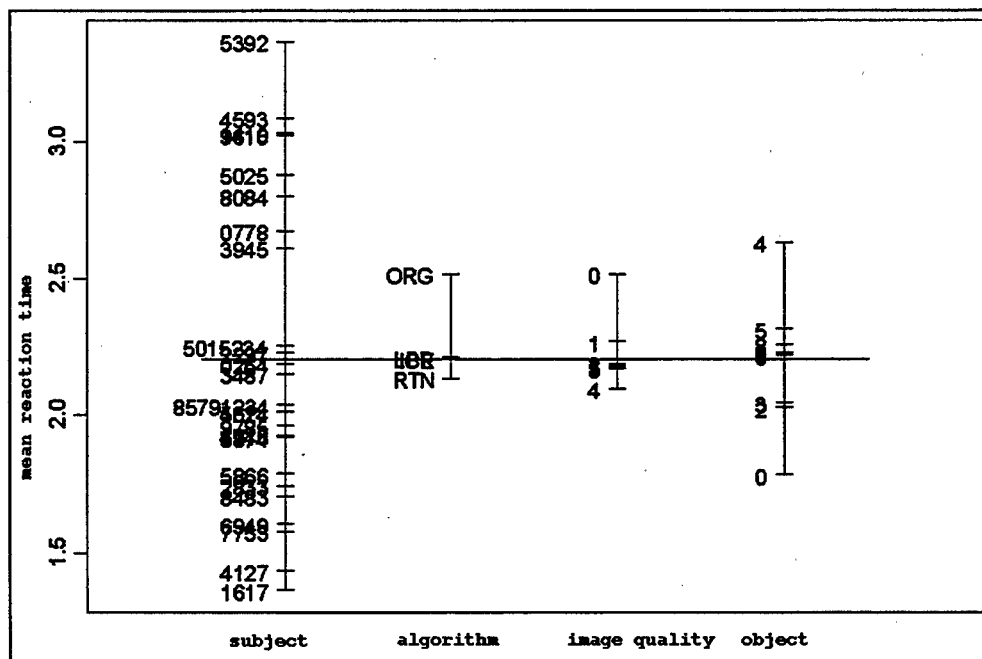


**Figure 34 Mean Reaction Time by Factor, Simple Background**



Three main factors (algorithm, object, and subject) combined with each other in two-way interactions to affect the reaction times. A significant algorithm by subject interaction, and a subject by object interaction can be seen. No trend in the data can be discerned, so the graphs are not included. There are no other significant interactions. There is no trend observed in any of the reaction time data.

The only exception is at image quality three, the reaction time significantly increased for ICE (Figure 35). The sample size is ten percent of both RTN and LBR. Each subject saw only three images compressed with ICE at image quality three. A paired comparison using Bonferroni's method was used to check for significance between RTN and ICE. Using a 0.01 level of significance ( $Z_{\frac{\alpha}{3}} = 2.7131$ ) there is significance only at image quality level three (Table 14). A 0.05 level of significance ( $Z_{\frac{\alpha}{3}} = 3.1280$ ) does not alter the results of the paired comparison.

image quality level	test stat
3	4.0505
4	0.1814
5	0.0874

**Table 14 Test Statistics for Paired Test of Reaction Time**

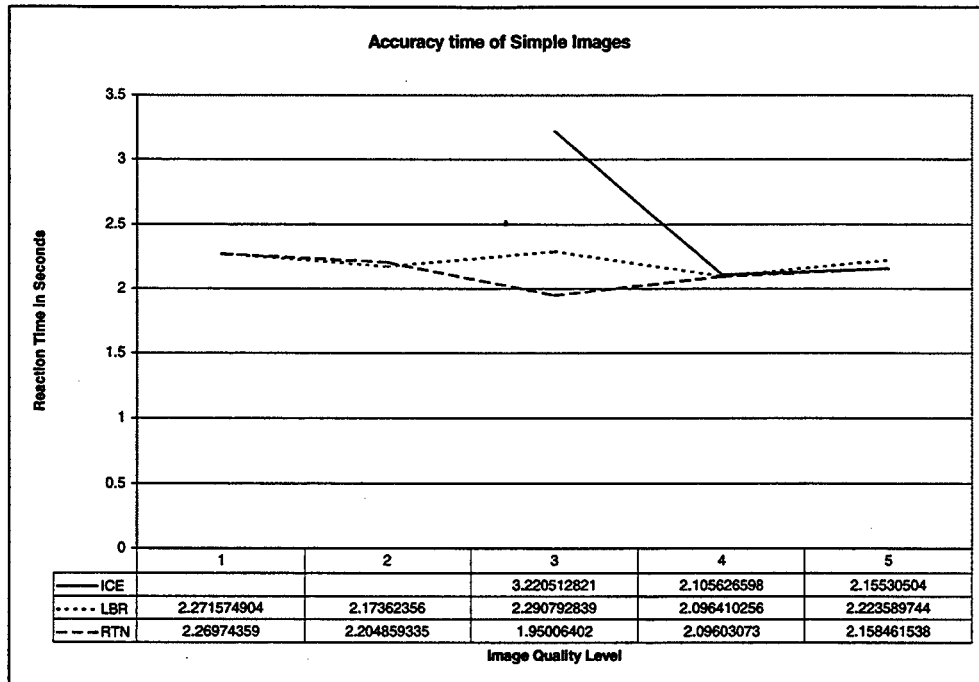


**Figure 35 Reaction Time by Algorithm, Simple Images**

## 2. Complex Images

A 3 x 6 x 10 x 5 ANOVA is calculated where the four factors are the type of algorithm (LBR, RTN, and ICE), the image quality (1, 2, 3, 4, 5, 6), the identity of the subject (unique number) and the target (SU, SE, MV, SP, ST). The dependent variable of the ANOVA is the average reaction time of each object type. The final model has been checked to verify that all significant interactions are included in the model. The ANOVA results are shown in Table 15.

	Df	Sum of Sq	Mean Sq	F Value	Pr(F)
Subject(s)	9	26.1238	2.902643	12.26126	0.0000000
Algorithm(a)	2	0.4827	0.241355	1.01953	0.3613066
Image quality(q)	5	11.9319	2.386386	10.08050	0.0000000
Object(o)	4	16.1080	4.027005	17.01075	0.0000000
s and a	18	7.4704	0.415024	1.75313	0.0271956
a and q	8	6.1242	0.765528	3.23372	0.0012744
a and q and o	60	19.5911	0.326519	1.37927	0.0344600
Residuals	693	164.0559	0.236733		
Residual standard error: 0.486552					

**Table 15 ANOVA of Reaction Time of Complex Images**

A non-significant effect for algorithm shows there is no difference in the reaction times when images are compressed with different algorithms (Figure 36). Algorithm is left in the model because of significant interaction terms involving algorithm. The effect of compression levels shows that as the image quality decreases (compression increasing) the reaction time of identifying objects increases. The image quality level zero is discussed in Chapter VII section B sub-section 2. The effect of object shows that the object type had an effect on reaction time. The subject main effect shows the subjects had an effect on reaction time. The subject effect on reaction time is less with the complex images due to the object selection for the test as discussed in Chapter VII section B sub-section 2.

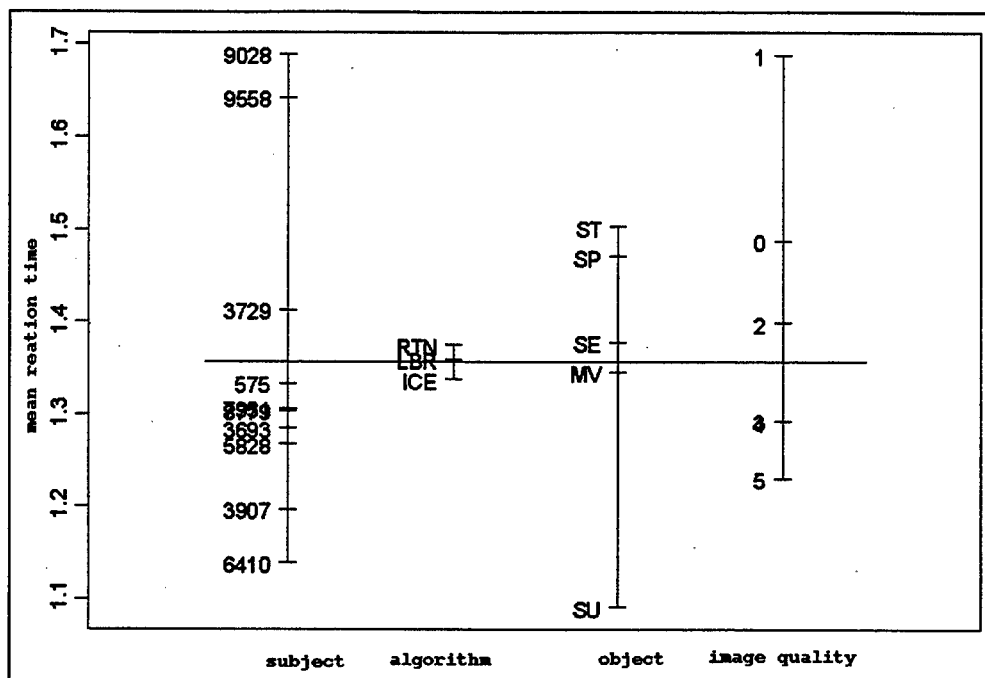


**Figure 36 Main effects on Time**

A significant subject algorithm interaction shows there is a significant difference in the subjects' reaction time in identifying different objects when compressed with the different algorithms. The graph shows no obvious trends and is therefore not included. The algorithm image quality interaction is significant. Additionally, a paired comparison gives a test statistic of less than 2.04 at all levels between RTN and ICE. The critical Z value is 2.8070 at a .01 level of significance and 2.2414 at a 0.05 level of significance. The algorithm and the compression ratio (image quality) interaction shows that as compression level increases (image quality decreasing) the reaction time increases (Figure 37). The three-way interaction between algorithm, compression level and object type was significant, but is not shown here.

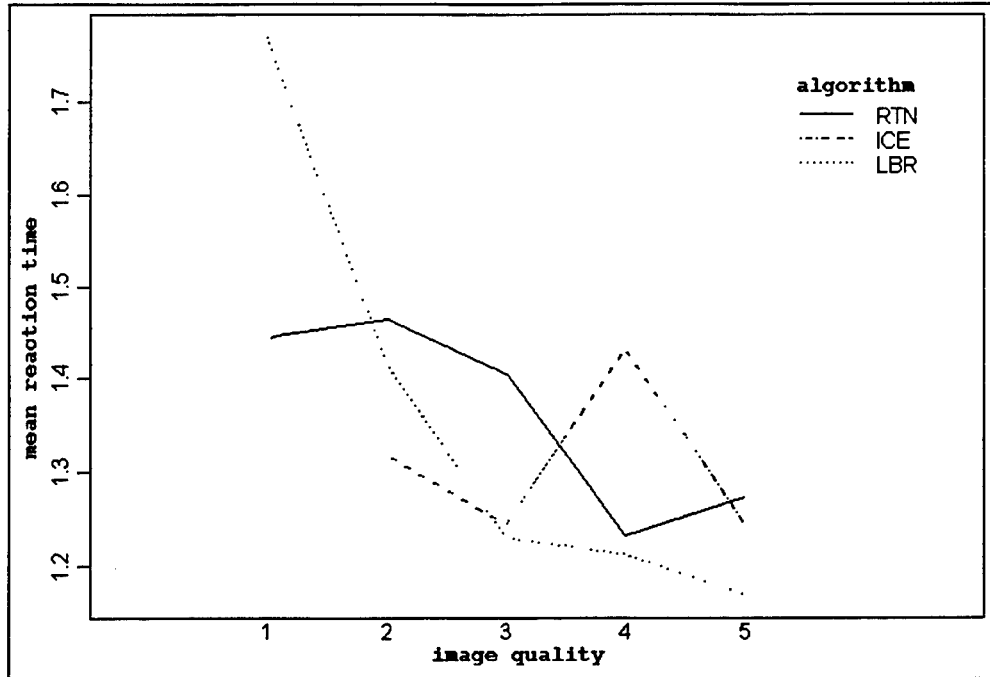


Figure 37 Reaction Time by Algorithm, Complex Images

#### D. PAIRED COMPARISON

In this analysis, subjects are shown two images and asked which is better, or are they the same. These pairwise comparison are evaluated using a Bradley-Terry model (David, 1988). The Bradley-Terry model is modified to take into account the option of the pair of images being judged the same. The model used in this thesis also contains a weight (wt) that represents the bias towards the first image presented. A weight greater than one indicates the first image is preferred. A weight less than one indicates the second image presented is preferred. This modified Bradley-Terry model generates scores (s) with the most preferred algorithm receiving the highest score. The scores are odds in the sense that the probability that algorithm  $i$  is preferred to algorithm  $j$  and  $i$  is

presented first: 
$$\frac{wt * s_i}{wt * s_i + s_j}.$$

The inputs for the model are two 3 by 3 matrices. The  $(i,j)^{\text{th}}$  element of the first matrix (A) is the total number of times that algorithm  $i$  is preferred to algorithm  $j$ . If the two are judged the same then one half is added to both the  $(i,j)^{\text{th}}$  and  $(j,i)^{\text{th}}$  elements. No image is ever compared to itself. The second matrix (A1) is the total number of times the algorithm presented first is preferred over the one presented second. Again, one half is added to each element in the case of the algorithms being judged equal.

For example, Table 16 contains the raw data from a comparison of the three algorithms. The table shows that if ICE is presented first, it is preferred 60 times when compared against LBR (First Image Preferred). If LBR is presented first, ICE is preferred 95 times (Second Image Preferred). ICE and LBR are judged equal 68 times when ICE is displayed first, and 70 times when LBR is displayed first (Images Equal).

	First Image Preferred			Second Image referred			Images Equal		
	ICE	LBR	RTN	ICE	LBR	RTN	ICE	LBR	RTN
ICE	0	60	63	0	95	113	0	68	92
LB	15	0	58	52	0	100	70	0	55
RT	15	24	0	25	67	0	52	56	0

**Table 16 Raw Data Matrixes**

The columns labeled A in Table 17 show the sum of the times ICE is preferred over LBR plus .5 for each time they are judged equal ( $60 + 95 + [68 + 70] * .5 = 224$ ). Of these 224 instances, 129 come from trials where ICE is displayed before LBR ( $60 + [68 + 70] * .5 = 129$ ).

	A			A1		
	ICE	LBR	RTN	ICE	LBR	RTN
ICE	0	224	248	0	129	135
LBR	136	0	213.5	84	0	113.5
RTN	112	146.5	0	87	79.5	0

**Table 17 Input Matrixes**

The results of the Bradley-Terry model from Table 17 are given in Table 18. The weight value is the bias value. The number is greater than one, therefore the first image is more likely to be preferred than the second image regardless of the algorithm. In this case, ICE is the preferred algorithm followed by LBR, then RTN.

	ICE	LBR	RTN
score	5.716	2.634	1.650
weight	1.551		

**Table 18 Bradley-Terry Sample Results**

### 1. Simple Images

Image quality one is entered into the Bradley-Terry model as a 2 by 2 matrix with RTN and LBR only. Table 19 shows the results from the simple images used in a pairwise comparison. The results are represented graphically in Figure 38. All numbers are rounded to three decimal places. RTN is preferred over LBR at all but the least compressed level. ICE is preferred over RTN and LBR at all image quality levels where ICE is present. As the image quality decreased and compression increased, the bias towards the first image being preferred increased.

Quality	ICE	LBR	RTN	Weight
1	na	1.368	8.632	4.475
2	5.526	1.345	3.129	2.134
3	6.141	1.230	2.559	1.814
4	5.289	1.984	2.727	1.613
5	5.027	2.715	2.258	1.607

**Table 19 Bradley-Terry Simple Image Scores**

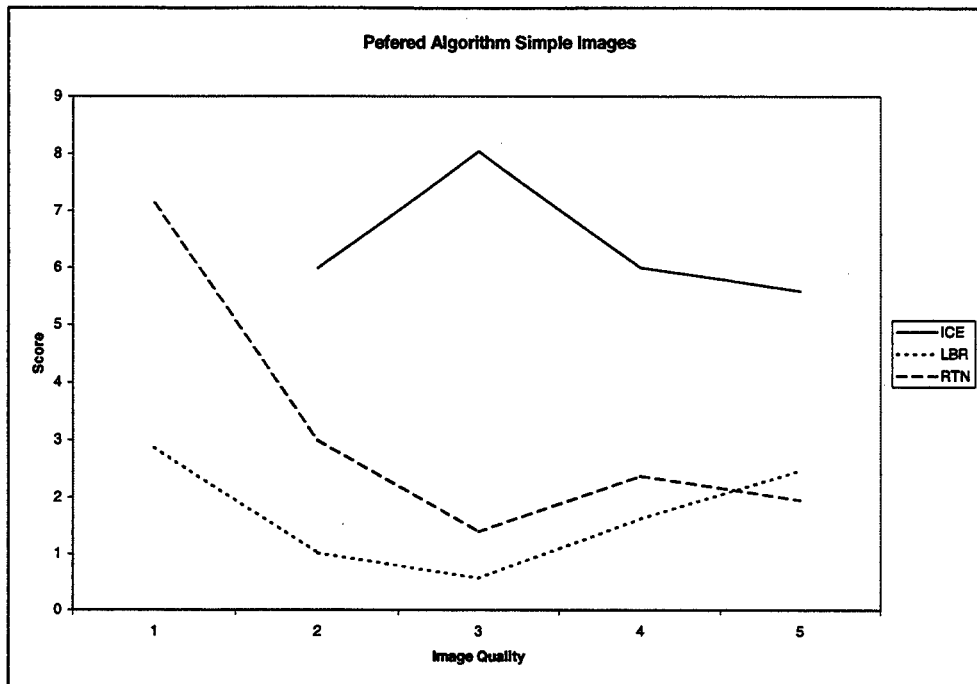


**Figure 38 Pairwise Comparison Scoring of Simple Images**

## 2. Complex Images

ICE is not compared against RTN and LBR due to the software limit at the lowest image quality, or highest compression ratio. ICE is preferred over both RTN and LBR in image qualities five down to quality two (Table 20). As the image quality decreased, ICE is preferred at an increasing rate (Figure 39). The bias towards favoring the first image presented increased again as the image quality decreased. There is one exception to the increasing bias: at image quality four, the bias dropped slightly.

RTN is judged better than LBR at all but the highest image quality. The analysis of the comparison between RTN and LBR is done as a 2 by 2 matrix with 4 points added to both the A and A1 matrixes. The diagonals of both A and A1 matrixes are set to zero. The addition is made to lower the bias towards the first image. The addition of the original values does not change the overall ranking significantly. The change in ranking



score is less the 0.001 as the addition value is changed. This addition does reduce the bias toward the first image; 10.140 is a lower bound for the true value.

Quality	ICE	LBR	RTN	Weight
1	na	0.563	9.437	10.140
2	9.223	0.226	0.551	4.339
3	7.182	1.112	1.707	1.948
4	6.981	1.322	1.696	1.315
5	5.716	2.634	1.650	1.552

**Table 20 Bradley-Terry Complex Image Scores**

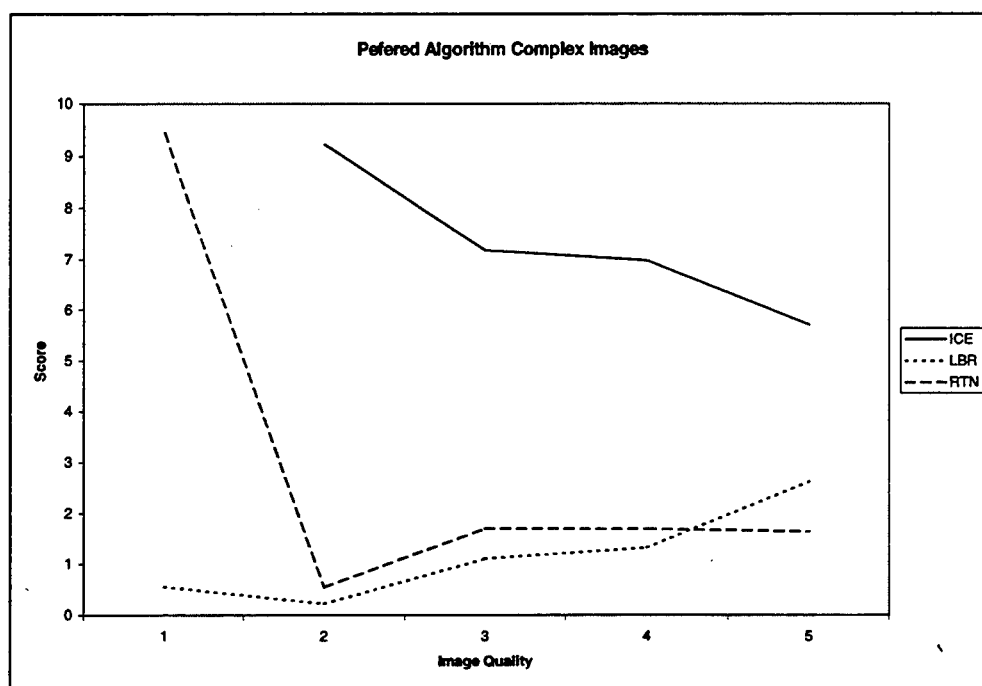


**Figure 39 Pairwise Comparison Scoring of Complex Images**

## VIII. CONCLUSION

This thesis compares the three lossy algorithms Interim Low Bit Rate, Titian ICE, and Radiant TIN at compression ratios greater than the current DoD compression standard (NITF) can achieve. The goal of this thesis is to determine whether LBR or ICE performs significantly better than RTN. Three experiments are conducted to determine the effect of these compression algorithms on target detection, target identification, and reaction time. Additionally, the subjects are shown two compressed images and asked to select a preferred image. All three algorithms compress images to at least a 100 to 1 compression ratio, exceeding NITF's maximum compression ratio.

The algorithm and compression ratio did not affect the identification of ships in a simple background. There are large individual differences in the respective subjects' abilities to identify the ships. In attempting to identify ships, an increase towards greater accuracy could be gained by increasing training of the subjects. Additional testing is recommended with simple image backgrounds using commonly known target objects, such as cars, to reduce the effect of subject training and knowledge on the accurate identification of targets. The identification of cars in the complex background shows that ICE performs best followed by RTN then LBR. However, there is no statistically significant difference between ICE and RTN. RTN consistently performs better than LBR in target detection. It also performs better than LBR in the identification and subjective rankings of both the complex and simple images. There is no statistically significant difference in reaction times based on compression algorithms. The only result

consistent throughout the reaction time testing is that as the compression ratios increase the subjects' reaction times slowed.

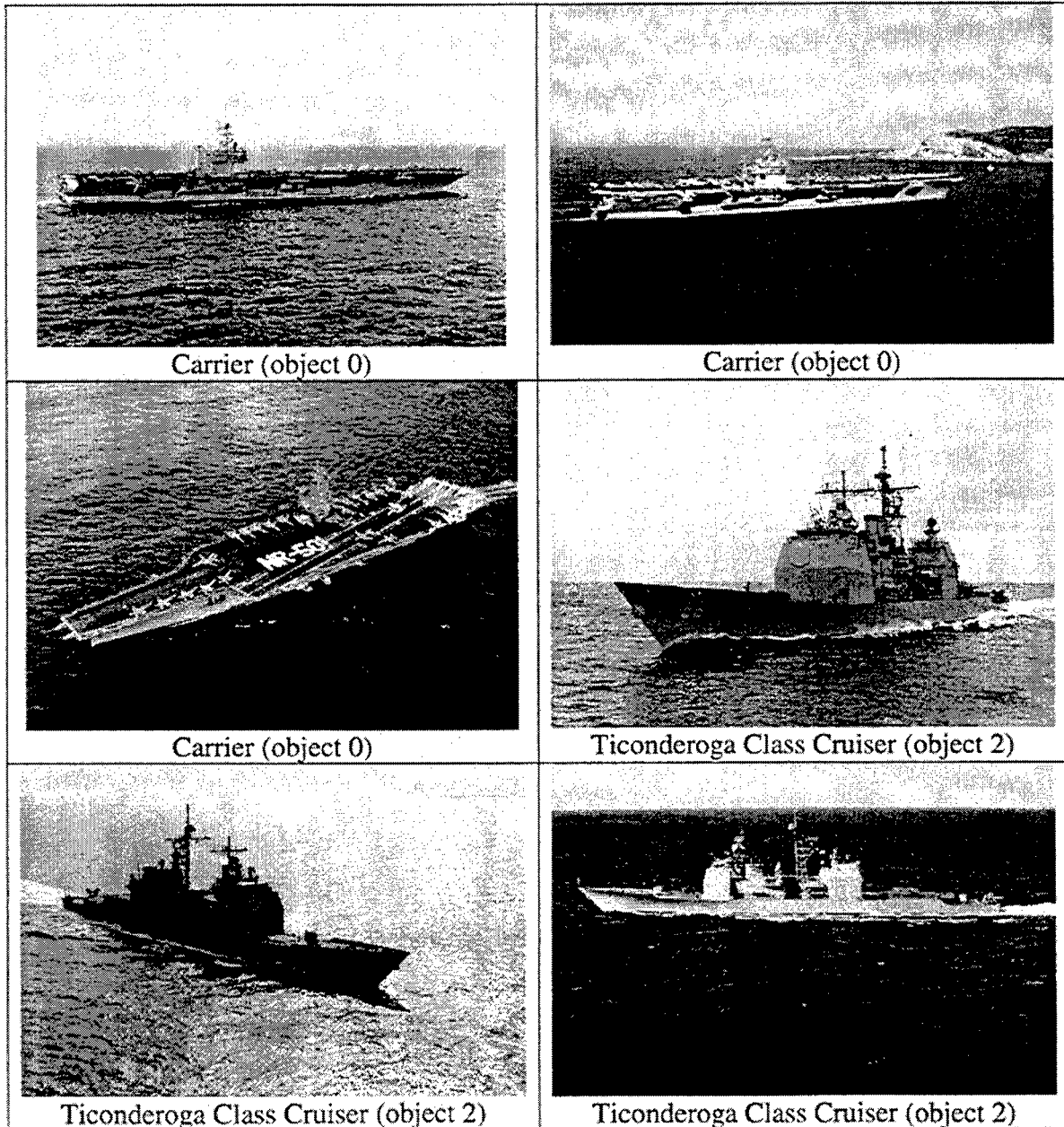
The results of subjective rankings of image quality are consistent across both the simple and complex background test images. ICE is the algorithm subjectively preferred over either of the other algorithms at all compression ratios. RTN is consistently preferred over LBR with the exception of the lowest compression ratios. This effect is also observed in the accuracy testing. The difference is LBR's ability to compress images with less noticeable changes at the lowest compression ratios and thus does not invalidate the overall preference of RTN.

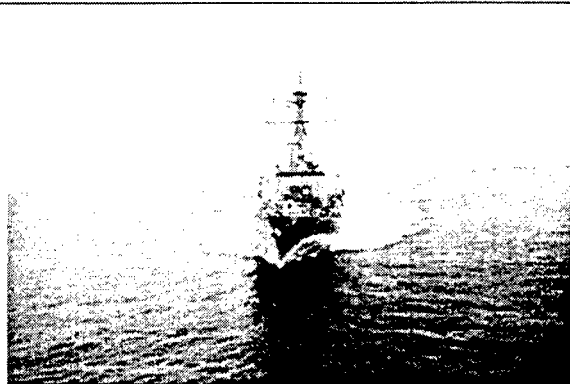
ICE's overall performance is better than RTN; however the difference between the two algorithms is not statistically significant. Additionally, the ICE compression software is limited by its graphical user interface of compression ratios of 100 to 1; RTN does not have this limitation. Furthermore, the Navy already has the proprietary rights to RTN and would not have to purchase a new algorithm. RTN is the recommended compression algorithm. Any future testing should include the NITF 2.0 standard that was released at the completion of this study, and ICE should be reevaluated if the 100 to 1 software limitation is removed.

## APPENDIX A. TEST IMAGES

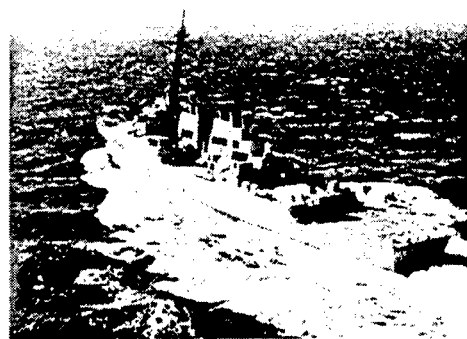
The following are the images for the accuracy and reaction time test. Both the simple background and complex background image sets are included.

### A. SIMPLE IMAGES

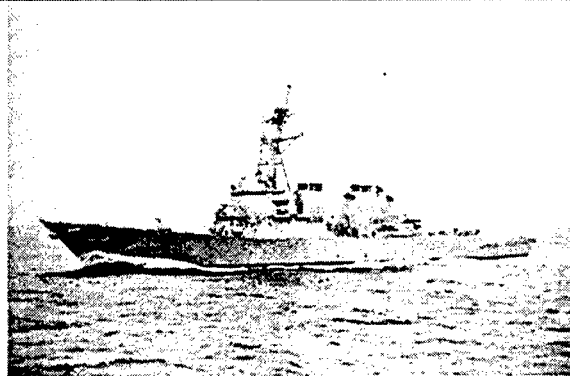




Arleigh Burke Class Destroyer (object 3)



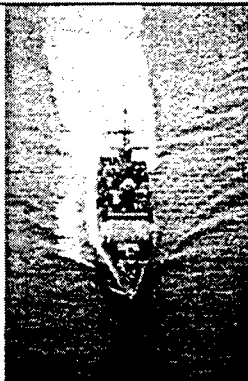
Arleigh Burke Class Destroyer (object 3)



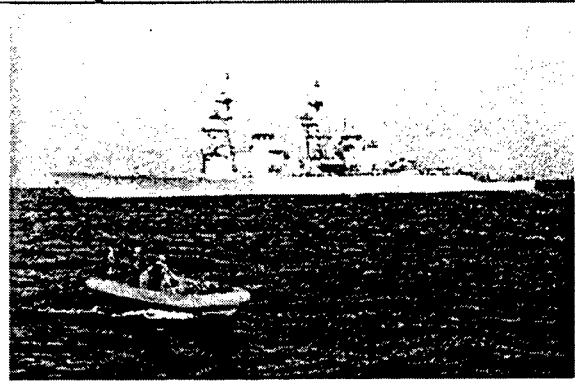
Arleigh Burke Class Destroyer (object 3)



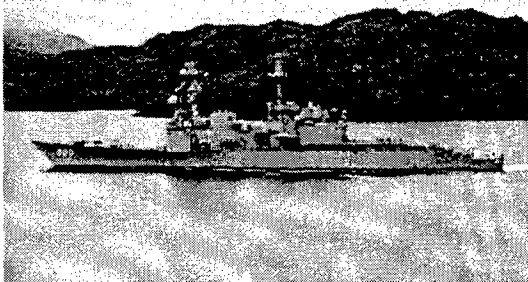
Arleigh Burke Class Destroyer (object 3)



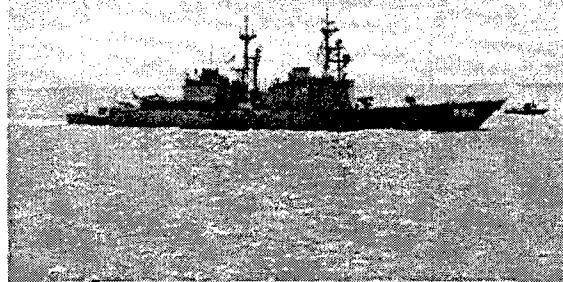
Spruance Class Destroyer (object 4)



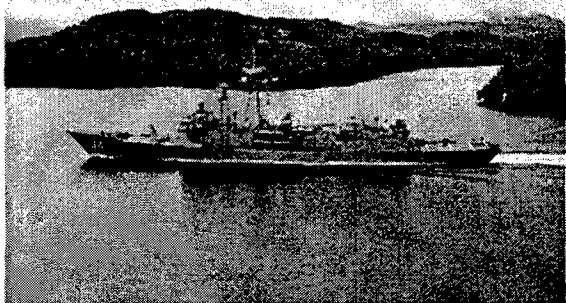
Spruance Class Destroyer (object 4)



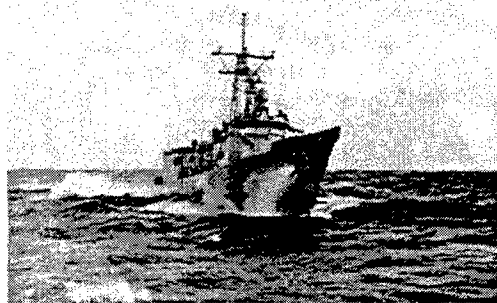
Spruance Class Destroyer (object 4)



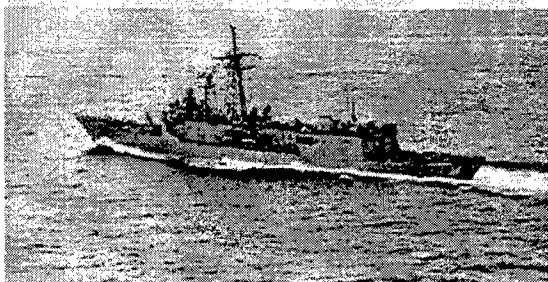
Spruance Class Destroyer (object 4)



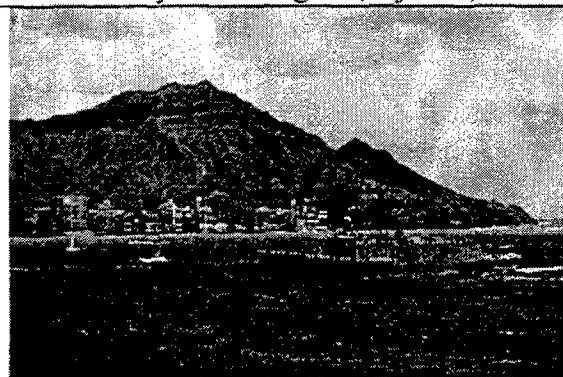
Perry Class Frigate (object 5)



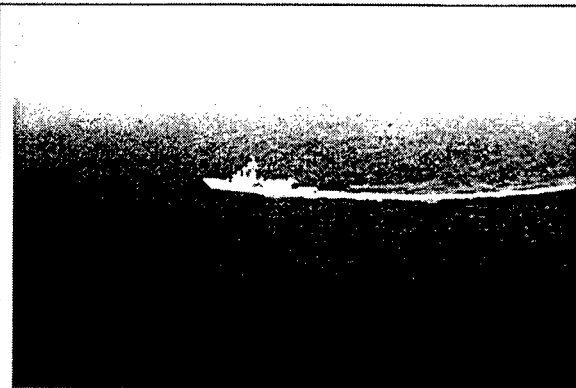
Perry Class Frigate (object 5)



Perry Class Frigate (object 5)



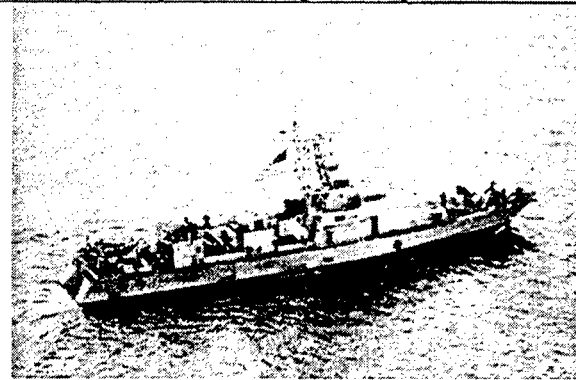
Perry Class Frigate (object 5)



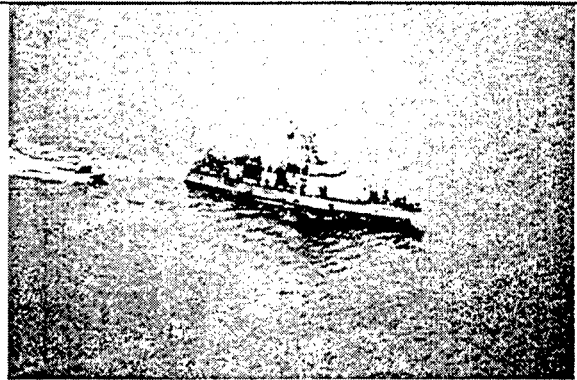
Perry Class Frigate (object 5)



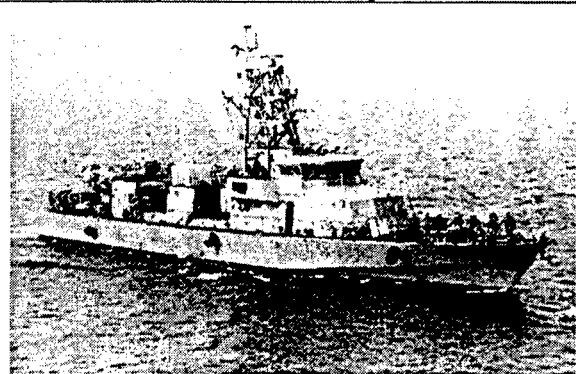
Perry Class Frigate (object 5)



Cyclone Class (object 6)



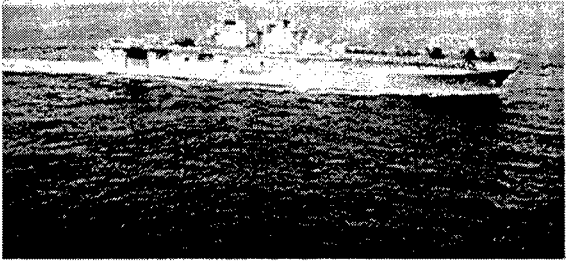
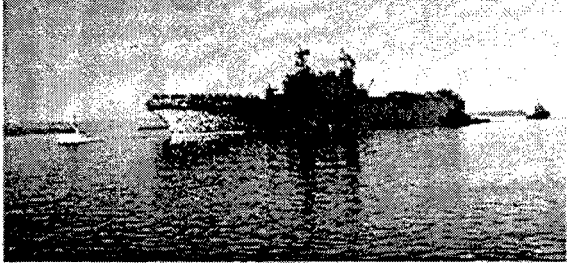
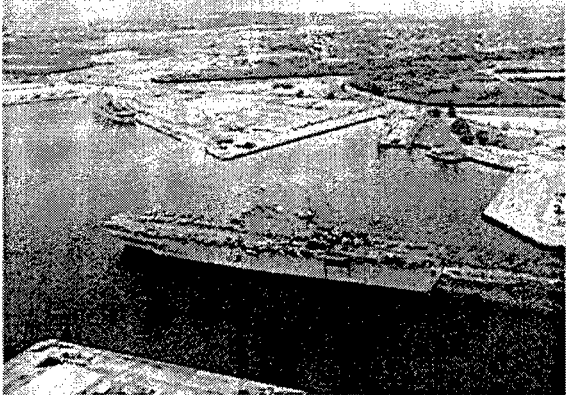
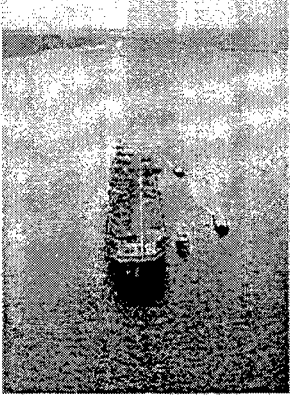
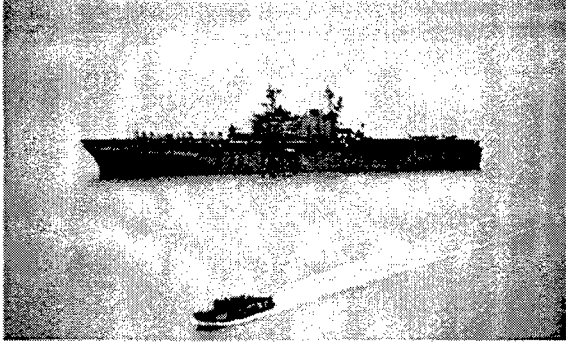
Cyclone Class (object 6)



Cyclone Class (object 6)



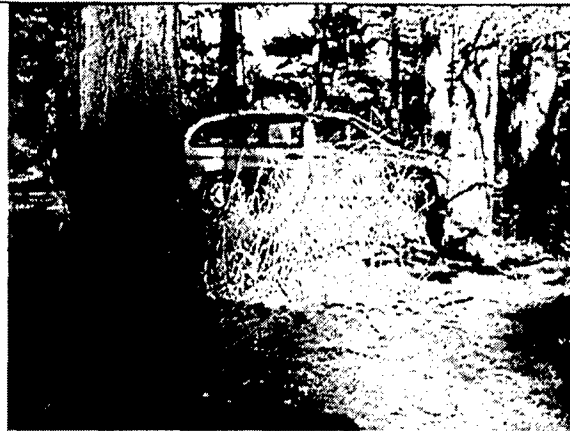
Wasp Class (object 8)

	
	
	<p>No other images</p>

## B. COMPLEX IMAGES

The following images were used in the complex background accuracy and reaction time test.





Mini Van (object MV)



Mini Van (object MV)



Mini Van (object MV)



Mini Van (object MV)



Sedan (object SE)



Sedan (object SE)



Sedan (object SE)



Sedan (object SE)



Sports Car (object SP)



Sports Car (object SP)



Sports Car (object SP)



Sports Car (object SP)



Station Wagon (object ST)



Station Wagon (object ST)



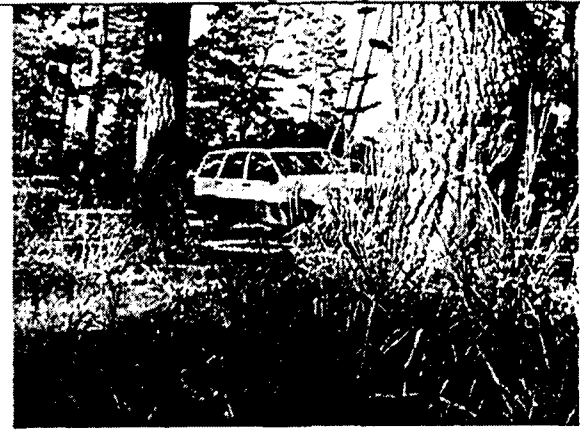
Station Wagon (object ST)



Station Wagon (object ST)



Sports Utility Vehicle (SU)



Sports Utility Vehicle (SU)



Sports Utility Vehicle (SU)



Sports Utility Vehicle (SU)



## APPENDIX B. BRADLEY-TERRY MODEL

The following code is the code that was used in S-Plus 4.0 to implement the Bradley-Terry pairwise comparison model.

```
function(A, A1, tot = 10, add = 0)
{
# fname is wts1
# A is the win-loss matrix; A1 is win-loss matrix for the
# row index being the host team or the first presented object;
# w1 is the set of Ford weights w/o consideration for home team
# or order of presentation; w is the weight set adusted for such
# considerations and then th is the odds multiplier for first
# presentation or host team..
# weights scaled so that total weight is 10. This may be over-
# ridden in the call by using another value.
  k <- dim(A)[1]
  mat <- matrix(1, k, k) - diag(k)
  A <- A + add * mat
  A1 <- A1 + 0.5 * add * mat
  AA <- apply(A, 1, sum)
  N <- A + t(A)
  w <- AA/apply(N, 1, sum)
  w <- (tot * w)/sum(w)
  ep <- 1e-006
  w0 <- w      # now we can find the raw Ford weights
  repeat {
    ww <- w
    tt <- outer(w, w, "+")
    w <- AA/apply(N/tt, 1, sum)
    w <- (tot * w)/sum(w)
    if(max(abs(w - ww)) < ep)
      break
  }
# the raw weights are use as a 'warm' start
# for the adjusted weights
  w1 <- w
  th <- 1
  A11 <- sum(A1)
  N1 <- A1 + t(A - A1)
  repeat {
```

```

th0 <- th
ww <- w
NN <- outer(th * w, w, "+")
tt <- apply(N1/NN, 1, sum)
th <- A11/sum(w * tt)
tt <- tt * th
w <- AA/tt
w <- (tot * w)/sum(w)
if(abs(th - th0) < ep) {
  if(max(abs(w - ww)) < ep) {
    break
  }
}
# if((abs(th - th0) < ep) && (max(abs(w - ww)) < ep)) break
}
# output has three rows. The first contains the raw weights,
# the second contains the adjusted weights, the third has theta.
z <- rbind(w1, w, c(th, rep(0, k - 1)))
z
}

```

## REFERENCES

- Beser, N.D., "Space Data Compression Standards," *Johns Hopkins APL Technical Digest*, v.15, pp. 206-223, 1994.
- Bray, J., *The Communications Miracle*, Plenum Publishing, 1995.
- Briggs, R.W. and Goldberg, J.H., "Battlefield Recognition of Armored Vehicles," *Human Factors*, v.37, pp. 596-610, September 1995.
- Brower, B.V., "Low-bit Rate Image Compression Evaluations," *SPIE*, v.2239, pp. 190-198, 1994.
- Caputo, G., "The Role of the Background: Texture Segregation and Figure-Ground Segregation," *Vision Research*, v.36, pp. 2815-2826, 1996.
- David, H.A., *The Method of Paired Comparisons*, 2d ed., Oxford University Press, 1988.
- González, J.G., Smith, M.J.T., Hontsh, I., Karam, L., Namuduri, K., and Szu, H., "Perceptual Image Compression for Data Transmission on the Battlefield," *SPIE*, v.3387, pp. 56-65, April 1994.
- Handel, M. I., *Masters of war : Sun Tzu, Clausewitz, and Jomini*, Frank Cass, 1992
- Holzman, G.J. and Pehrson, B., *The Early History of Data Networks*, IEEE Press, 1995.
- Huffman, D.A., "A Method for the Construction of the Minimum-Redundancy Codes," *Proceedings of the IRE*, pp. 1098-1101, September 1952.
- ISOA, APL, "TID 3.0 Documentation," ISOA, APL, pp. 23, April 1995.
- Jayant, N., Johnston, J., and Safranek, R., "Human Vision, Visual Processing, and Digital Display IV," *SPIE*, v.1913, pp. 168-178, February 1993.
- "JPEG image compression FAQ," [<http://www.cis.ohio-state.edu/hypertext/faq/usenet/jpeg-faq/top.html>], June 1998.
- Joint Chiefs of Staff, *Joint Vision 2010*, Government Printing Office, Washington, D.C., July 1996.
- Joint Chiefs of Staff, *Concept for Future Joint Operations: Expanding Joint Vision 2010*, Government Printing Office, Washington, D.C., May 1997.



Lan, A. and Reitz, J., *Detailed Implementation Guidelines for the Interim Low Bit Rate Compression System*, Eastman Kodak Company Commercial and Government Systems, 27 November 1996.

Masini, G., *Marconi*, Marsilio Publishers, 1996.

Moeller, P. and Hurlbert, A., "Interaction Between Colour and Motion in Image Segmentation," *Current Biology*, v.7, pp. 105-111, February 1997.

Muolo, M., *Space Handbook: A War Fighters Guide to Space*, Air University Press. Maxwell AFB, AL., 1993.

National Academy of Sciences, "The Evolution of Untethered Communications." [<http://www.nap.edu/readingroom/books/evolution/1.html>]. 1997.

National Imagery and Mapping Agency [NIMA], "What is the NITFS?" [[164.214.2.59/NITFS/intro.html](http://164.214.2.59/NITFS/intro.html)], 1999.

Paragon Imaging, "Imagery on Open Systems: The Role of the National Imagery Transmission Format." [[http://www.paragon.com/nitf\\_whitepaper.html](http://www.paragon.com/nitf_whitepaper.html)], 1999.

Rabbani, M. and Jones, P.W., *Digital Image Compression Techniques*, v.TT7, SPIE-The International Society for Optical Engineering, 1991.

Reiter, E., "Wavelet Compression of Medical Imagery," *Telemedicine Journal*, v.2, pp. 131-137, 1996.

Rubenstein, B. and Sagi, D., "Spatial Variability as a Limiting Factor in Texture-Discrimination Tasks: Implications for Performance Asymmetries," *Journal for Optical Society of America*, v.7, pp. 1623-1642, September 1990.

Sanford, M.A., *An Analysis of Data Compression Algorithms used in the Transmission of Imagery*, Master's Thesis, Naval Postgraduate School, Monterey, California, June 1995.

Venkataraman, S. and Farrelle, P.M., "Low bit rate compression using recursive techniques," *SPIE*, v.2239, pp. 214-223, April 1994.

Waller, H.T., *The HAE UAV and Dynamic Retasking by Tactical Commanders*, Master's Thesis, Naval Postgraduate School, Monterey, California, June 1996.

## BIBLIOGRAPHY

Ahumada Jr., A.J. and Horng R., "De-blocking DCT Compressed Images," *SPIE*, v.2179, pp. 109-116, February 1994.

Applied Physics Laboratory, Report VSE(2)-97-134, *Evaluation of the Radiant Tin and the National Imagery Transmission Format Standard (NITFS) Interim Low Bit Rate Compression Routines*, by V.C. Walton, 2 December 1997.

Applied Physics Laboratory, Report FS-94-048, *Space and Electronic Warfare Program: Best of Breed Data Compression Evaluation Criteria*, by N.D. Beser and A.A. Tomko, March 1994.

Barten, P.G.J., "Spatio-Temporal Model for the Contrast Sensitivity of the Human Eye and its Temporal Aspects," *SPIE*, v.1913, pp. 2-14, February 1993.

Beser, N.D., "Image Data Compression Metrics," *AIAA-93-4513-CP*, AIAA, pp. 292-303, 1993.

Biederman, I., Glass, A.I., and Stacy Jr., E.W., "Searching for Objects in Real-World Scenes," *Journal of Experimental Psychology*, v.97, pp.22-27, 1973.

Dember, W.N., *Psychology of Perception*, Holt, Rinehart, and Winston, 1979.

van Dijk, A.M. and Martens, J.-B., "Feature-Based Image Compression with Steered Hermite Transforms," *IEEE Proceedings*, v.I., pp. 205-208, September 1996.

Efstratiadis, S.N. and Strintzis, M.G., "Hierarchical Prioritized Predictive Image Coding," *IEEE Proceedings*, v.I., pp. 189-192, September 1996.

Finamore, W.A. and de A. Leister, M., "Lossy Lempel-Ziv Algorithm for Large Alphabet Sources and Applications to Image Compression," *IEEE Proceedings*, v.I., pp. 225-228, September 1996.

Friedlander, N., Schlueter, K., and Mantei, M., "Bullseye! When Fitts' Law Doesn't Fit," *CHI'98*, pp. 257-264, April 1998.

Gale, A., "DCT Basis Function Visibility: Effects of Viewing Distance and Contrast Masking," *SPIE*, v.2179, pp. 99-108, February 1994.

Gao, Q., "Man-made Object Recognition Based on Visual Perception," *Journal of Electronic Imaging*, v.7, pp.104-110, January 1998.

Kia, O.E. and Doermann, D.S., "Structure-Preserving Document Image Compression," *IEEE Proceedings*, v.I, pp. 193-196, September 1996.

Klein, S.A., Silverstein, A.D., and Carney, T., "Relevance of Human Vision to JPEG-DCT Compression," *SPIE*, v.1666, pp. 200-215, February 1992.

La, G. and Yew, T., "Image Compression Using Partitioned Iterated Function Systems," *SPIE*, v.2186, pp. 122-133, February 1994.

Li, Jiankun, Li, Jin, and Kuo, C.-C.J., "An Embedded DCT Approach to Progressive Image Compression," *IEEE Proceedings*, v.I, pp.201-204, September 1996.

Lin, C.C. and Pease, D.J., "A Bracket Classified Coding Scheme for Image Compression," *IEEE Proceedings*, v.I, pp. 209-212, September 1996.

Longhini, J.M. and Scott, S.J., *Digital Video Transmission from the P-3C to Beyond Line of Sight Destinations*, Master's Thesis, Naval Postgraduate School, Monterey, California, September 1995.

Ma, K., "Modified Absolute Moment Block Truncation Coding," *IEEE Proceedings*, v.I, pp. 197-200, September 1996.

Muller, F., Illgner, K., and Menser, B., "Embedded Laplacian Pyramid Image Coding Using Conditional Arithmetic Coding," *IEEE Proceedings*, v.I, pp. 221-224, September 1996.

Neisser, U., *Cognitive Psychology*, Appleton-Century-Crofts, 1967.

Pappas, T.N., Michel, T.A., and Hinds, R.O., "Supra-Threshold Perceptual Image Coding," *IEEE Proceedings*, v.I, pp 237-240, September 1996.

Peyton Jr., W.M., *Multiresolution Image Recognition Using the Wavelet Transform*, Master's Thesis, Naval Postgraduate School, Monterey, California, June 1996.

Peterson, H.A., "An Improved Detection Model for DCT Coefficient Quantization," *SPIE*, v.1913, pp.191-201, February 1993.

Reed, T.R., "Image Sequence Coding Using Spatial/Spatial-Frequency Representations," *SPIE*, v.1666, pp. 216-225, February 1992.

Roufs, J.A.J., Koselka V.J.F., and van Tongeren, A.A.A.M., "Global Brightness Contrast and the Effect on Perceptual Image Quality," *SPIE*, v.2179, pp. 80-89, February 1994.

Safranek, R.J., "A JPEG Compliant Encoder Utilizing Perceptually Based Quantization," *SPIE*, v.2179, pp. 117-127, February 1994.

Shires, D.R., Holly, F.F., and Harnden, P.G., "High-Ratio Bandwidth Reduction of Video Imagery for Teleoperation," *SPIE*, v.1903, pp. 236-245, February 1993.

Sinha, D. and Dougherty, E.R., *Introduction to Computer-Based Imaging Systems*, v.TT23, SPIE Optical Engineering Press, 1998.

Sloan, A.D., "Low Bit Rate Fractal Image Coding," *SPIE*, v.2239, pp. 210-213, April 1994.

Stager, P., "Locating Crash Sites in Simulated Air-to-Ground Visual Search," *Human Factors*, v.20, pp. 453-466, August 1978.

Su, J.K. and Mersereau, R.M., "Coding Using Gaussian Mixture and Generalized Gaussian Models," *IEEE Proceedings*, v.I, pp.217-220, September 1996.

Terwilliger, R.B. and Polson, P.G., "Relationships Between Users' and Interfaces' Task Representations," *CHI'97*, pp. 99-106, March 1997.

Watson, A.B., "DCT Quantization Matrices Visually Optimized for Individual Images," *SPIE*, v.1913, pp. 202-216, February 1993.

Weiman, C.F.R., "Video Compression by Matching Human Perceptual Channels," *SPIE*, v.2239, pp.178-189, April 1994.

Wolfe, J.M., "Visual Search in continuous, Naturalistic Stimuli," *Vision Res.*, v.34, pp.1187-1195, 1994.

Wolfe, J.M., "'Effortless' Texture Segmentation and 'Parallel' Visual Search and *not* the Same Thing," *Vision Res.*, pp.757-763, 1992.

Yfantis, E.A. and Au, M., "An Image Compression Algorithm based on Kriging," *SPIE*, v.1903, pp. 215-227, February 1993.

Yoo, K.-H. and Choi, J., "A Model Based Method for the Quantizer Assignment of JPEG-Like Coders," *IEEE Proceedings*, v.I, pp. 213-216, September 1996.

Young, R.A., "Oh Say, Can You See? The Physiology of Vision," *SPIE*, v.1453, pp. 92-121, March 1991.



## INITIAL DISTRIBUTION LIST

1. Defense Technical Information Center ..... 2  
8725 John J Kingman Rd, STE 0944  
Ft. Belvior, VA 22060-6218
2. Dudley Knox Library ..... 2  
Naval Postgraduate School  
416 Dyer Rd  
Monterey, CA 93940-5000
3. Lt. Christopher Bodine ..... 4  
2519 Sea Breeze Ct  
Merced, CA 95340
4. Dr. Richard Rosenthal ..... 1  
Naval Postgraduate School  
Code OR/RI  
1588 Cunningham Road  
Monterey, CA 93943
5. Dr. William Krebs ..... 1  
Naval Postgraduate School  
Code OR/KB  
1588 Cunningham Road  
Monterey, CA 93943
6. Dr. Lynn Whitaker ..... 1  
Naval Postgraduate School  
Code OR/WH  
1588 Cunningham Road  
Monterey, CA 93943
7. Dr. Robert Reed ..... 1  
Naval Postgraduate School  
Code OR/RE  
1588 Cunningham Road  
Monterey, CA 93943

8. William C. Walton .....	2
The Johns Hopkins University	
Applied Physics Laboratory	
Bldg 25-160	
11100 Johns Hopkins Rd.	
Laurel MD 20723-6099	